A Quantitative Analysis of Phyllotactic Patterns in *Thuja occidentalis* (Eastern White Cedar) at the Level of the Shoot Apical Meristem

A Thesis

Submitted to the Graduate Faculty

in Partial Fulfillment of the Requirements

for the Degree of

Master of Science

in the Department of Biology

Faculty of Science

University of Prince Edward Island

Xiaofeng Yin 殷晓泓

Charlottetown, Prince Edward Island

April, 2009

Your file Votre référence
ISBN: 978-0-494-49853-8
Our file Notre référence
ISBN: 978-0-494-49853-8

SIGNATURE PAGES

iii-iv

REMOVED

Abstract

Phyllotaxis is the study of the arrangement of primordia on the shoot apical meristem or mature organs on the stem. Phyllotactic patterns can change during the ontogenetic process and is called pattern transition. The main goal of this study is to examine different phyllotactic and transition patterns of the seedlings of *Thuja occidentalis*. Scanning electron and optical microscopy were used to examine dissected shoot tips of seedlings and take measurements of a variety of parameters. Four phyllotactic patterns were observed on the main stem of *T. occidentalis*: tetracussate, tricussate, (3, 5) spiral and decussate. Therefore, 4 types of phyllotactic pattern transitions were documented: tetracussate to decussate, tetracussate to tricussate, tricussate to (3, 5) spiral and (3, 5) spiral to decussate. Only 1 phyllotactic pattern was observed on the side branches of *T. occidentalis*: decussate. For each phyllotactic pattern, the following phyllotactic parameters were measured or calculated using histological techniques: divergence angle, plastochrone ratio, leaf insertion angle, parameter Γ and apical angle of the shoot apical meristem. The results from histological techniques indicate that: divergence angle, plastochrone ratio and leaf insertion angle fit with their empirical ranges for all the patterns; divergence angle and plastochrone ratio fit with some theoretical models for the (3, 5) spiral pattern of the main stem; parameter Γ only matched the theoretical prediction for the (3, 5) spiral pattern of the main stem; using $\Gamma = \sqrt{(l_1 l_2)}/R_0$ is a better way to calculate parameter Γ. This study is the first to use a scanning electron microscopy three-dimensional reconstruction method to study the shoot apical meristem at an early stage of development. Four new phyllotactic parameters were introduced: volume of the shoot apical meristem, surface area of the shoot apical meristem, projected area of the shoot apical meristem

and height of the shoot apical meristem. The results from the scanning electron microscopy three-dimensional reconstruction method indicate that: different phyllotactic patterns observed on *T. occidentalis* are not significantly different for these 4 parameters; the assumption that the shoot apical meristem can be approximated as a cone may not be valid. The results from histological techniques and scanning electron microscopy three-dimensional reconstruction method combined indicate that: the apical angle of the shoot apical meristem decreased significantly as the seedlings of *T. occidentalis* grow and undergo pattern transitions in both main stem and side branches.

Acknowledgments

I would like to first thank my parents, Jia Yin and Di Chen. Their love, support and encouragement were priceless to help me to complete this degree. This thesis is dedicated to them.

I would like to thank my supervisor Dr. Christian Lacroix. The completion of this thesis would have been impossible without his help. I always said to myself that: "you are very very lucky to have Chris as your supervisor, not a lot of students have that chance!" His suggestions and comments were always very helpful. Whenever I had a question, he always responded very quickly. I really appreciated his detail corrections of my manuscripts (even the acknowledgements part), whether for content or grammar. He also showed great personality as a friend and a role model. For those who know him personally, I don't need to say anymore.

I would also like to thank my co-supervisor, Dr. Denis Barabé. His suggestions and comments were always very constructive to help me to complete this thesis. His great knowledge of phyllotaxis lit a torch to guide me in the dark. I also appreciated his help with arranging a tour in Montreal back in 2007.

I would also like to thank my supervisory committee member, Dr. Marina Silva for her valuable suggestions and comments on my manuscripts. I had learned a lot from her about how to write a scientific thesis. Also thanks to Dr. Roger Meicenheimer from Miami University for serving as my external examiner and Dr. Beata Zagórska-Marek from Wroclaw University for her critical

comments.

Special thanks to my fellow graduate student Laura Bourque. She always helped me in the lab and answered my stupid questions like "where is this?" while the stuff was only one inch from my hands. I would also like to thank honors students Matthew Allain and Sarah Weidhass and undergraduate student Ari Morgenthau for their help in the lab. Also special thanks to my friend in China Peng Guo for drawing the curves in Figure 7C.

Special thanks to Dr. Robert Haines, former graduate study coordinator of Faculty of Science, University of Prince Edward Island. His recommendation was essential for me to be accepted by the current graduate program. May you rest in peace!

In addition, there are a lot of individuals that I have had the honor of knowing or working with for the past years in the Department of Biology:

Kerry-Lynn Atkinson: who is a fellow graduate student. One thing that I notice about her is that she turns off the computer everyday while leaves the light on.

Gilbert Blatch: who is normally easily forgotten by the people around himebecause he is so quiet. But when you need to find something or fix something in the Duffy building, he will be the first one who comes to mind for help.

Beth Brown: who was a student in the Plant Diversity lab and later became my TA partner for the first year lab. She always did more work than me in the lab. I felt really guilty about this.

Colin Burgoyne: who was a graduate student in the lab when I first came. His unique laugh was one of my favorite things in the lab.

Robert Déziel: who is a graduate student in the lab. Right now he is 1 of the 3 graduate students using such a big lab. I'm very jealous about this!

Dr. Tracy Doucette: who once "stole" part of our lab bench and stored her stuff there. Although we didn't have a lot of chance to see each other, we do smile to each other every time.

Patrick Doyle: who I worked with as his lab TA for almost 3 years in the Plant Diversity lab. He knows everything about plants, whether it is in the lab or in the field. I have learned so many things working with him. He always talks plants, soccer, politics, or the most random trivial stuff. And whenever he talks in his office, you can hear him from the first floor. So if you are looking for him, just open your ears and follow the sound.

Sarah Foster: who was a student in my Plant Diversity lab and Microbiology lab and my TA partner in the first year lab at the same time. Therefore, I saw her every Tuesday, Wednesday and Thursday afternoon last year. We worked together for 2 semesters so we had a chance to compete about who was the best (or worst) TA and this was voted on by the students. The first semester I

won (she claimed that I cheated) but the result was very close. The second time she won and almost every student voted for her. These results will be examples on next year's first year lab manual to teach students what is and how to do a chi-square test (and if you don't understand what a chi-square test is, I suggest that the acknowledgements is the only section you need to read for this thesis).

Edward Francis: who still holds the record for the longest time to complete an MSc program in the department history and I just heard a few days ago Dr. Hurta had to require to extend his program … again. The result of our competition for who finishes first is now very clear. I describe him as "drunk at night, sleep during the day". The only place you can find him on campus is the Wave, and that is only for pre-pre-party drink. Actually I do see him in the lab a lot in the morning and in the graduate students' room as well, and we chirp each other all the time, this is our way to show the love to each other. There was one time last summer when a friend and I went to Gahan's but it was full and the waitress told us we had to wait for 45 minutes. I told her "just tell Eddie Frank is here" and 5 minutes later we sat down and started to order food. About 2 weeks ago I heard Eddie would become a father in August. Congratulations and set the record as long as possible!

Dr. Donna Giberson: who is really easy-going and uses a "beaker" cup to drink. Her lectures are always very interesting.

Dr. Lawrence Hale: who was the chair of the department when I first came. I know him because I

was working as a TA for the course he taught. He is very patient and gentle when he talks to you, although a little bit fast for someone whose mother language is not English, such as me. I really want to thank him for giving me an opportunity to teach one of his lectures (DNA transcription I remember) in front of 300 students.

Terrie Hardwick: who I worked with as her lab TA in the first year lab. She was really nice to me (and everybody else) and working with her was a big pleasure. Although she calls me "trouble" all the time, I know she does love me. And if you smell anything good in the hall way of the Duffy building, it must be her lunch.

Dr. Natacha Hogan: who I first thought is an undergrad student then turned out to be a post-doc! We worked face to face for a long time.

Dr. Robert Hurta: who is currently the graduate study coordinator. Although he claims that he always works at his office on Saturdays, I have only seen him there once. Maybe it is because I always come very late.

Eva Jenkins: who was first an honor student and later became a graduate student. I was very jealous that she had that chance to go to South Africa last summer for her project.

Dr. James Kemp: who is considered the funniest professor by students. He has a bonus question in his exam: which following statement is correct and the choices include something like: the only

good plant is a boiled one on a plate with some vinegar and a fork; his course is better than shoveling snow in your drive way using a spoon, *et al.*

Whitney Kelly-Clark: who I went to Truro with 2 years ago for the Canadian Wide Science Fair. It was a really good trip and we stole big signs for the science fair as souvenirs together and brought them back. I still keep my sign and I believe she still keeps hers.

Dr. Christian Lacroix: you don't describe him twice!

Dr. Lawrence Liao: who was a professor when I first came and invited me to audit his lectures. That was very helpful for me to practice my listening skills for English. I remember he once forgot to take his boots with him while we were on a field trip so he had to wait for 2 hours while Pat explained everything to us.

William MacDonald: who was a technician in the lab and now is a vet student. The idea of writing this part of the acknowledgements, which turns out not that easy, was actually inspired from his thesis. Recently we became TA partners in the first year lab and it was a pleasure. We teased each other all the time in front of the students. I always got caught by him when I ate burgers and he teased me on that a lot and finally I said "I'm going to McDonald's to buy 100 big Macs and will just eat the lettuce". I was very happy that he was my partner because I know nothing about rats. And I think he was very happy that I was there too because he knows nothing about plants after he became a vet student.

Colleen MacDougall: who holds an annual cocktail party with Adam. When she told me she was transferring to another lab, I was shocked and missed her for a while. Hope I will see you this summer at home.

Adam MacLean: who holds an annual cocktail party with Colleen. He always holds his camera and takes picture when you are unprepared. Hope I will see you this summer at home too.

Eric Pass: who I worked with as his lab TA in the first year lab. I like to tease him because he will tease back something even funnier. We sometimes played badminton together, and of course I beat him big time.

Dr. Pedro Quijon: who I still don't know how to pronounce his last name. Although we don't talk too much, he seems to be a very nice person and students like him.

Elizabeth Rostant: who I worked with as her lab TA in the Microbiology lab. She is very nice and always welcomes me to her office to bug her and Terrie. I still owe her an alcohol lamp I have borrowed from her.

Bradley Scott: who is a graduate student in the lab. Our desks in the graduate students' are next to each other and he plays video games all the time there. That is probably why it took so long for me to finish my thesis because he distracted me too much. I hope Dr. Hurta will not see this part.

Kevin Shaughnessy: who is the biggest alcoholic in the lab. I remember one time I had to walk him home at 2 o'clock in the morning to make sure he was OK. We were also partners in badminton doubles and apparently I carried the team he dragged the team. Good luck on your new life in Halifax!

Dr. Marina Silva: who is always very busy. She told me she likes Chinese food a lot. I hope she meant non-Canadianized Chinese food. I also hope she likes my thesis and will not fail me.

Dr. Jennifer Slemmer: who organizes parties for graduate students and staff pretty much every week in her manor. We work on different sides of the lab, but I can hear her laugh all the time, mostly laugh at Kevin's stupid statements.

Dr. Marva Sweeney-Nixon: who always gives me snacks after the seminar is over, although I don't show up. She also lent me a calculator for my thesis, which I did return.

Dr. Kevin Teather: who asked me a question and then I messed up after my representation 2 years ago and now I have a good answer for that question. His recent seminar title was extremely interesting and I planned for more than half a year to attend, then it turned out I have to work for Pat at the same time. What a shame!

Jessy Livingston Thomas: who wanted to hear why my nickname is "strawberry" but I haven't had a chance to tell her.

Sarah Wisniewski: who was a student in the first year lab and Plant Diversity lab while I was the TA for both. She later became a TA for the first year lab. She is my favorite student because her answers were always right. Whenever I cannot find the answer key for the quiz, I just used her answer as the key. I still keep one of her drawings in the first year lab because it was just beautiful.

I remember when I just entered in the program, one day I carried my cedars in the lab and Dr. Hurta asked me what they were. I said those were the things that I would work on for the next 2 years and then he asked me again "2 years?" and then I said maybe a little bit more than 2 years. At that time I didn't want to spend more than 2 years to finish the program and wanted to get out of here as soon as possible. Right now, 2 and half years later, at the moment I am almost done, I have to say I changed my mind and I really want to stay but it is time to move on. The memory of the time I spent here is more than beautiful. I would like to thank my friends: Mohammad Altheiban, Sean Aylward, James Baglole, Hilary Buckley, Miriam Burchell, Jonathan Cooper, Daniel Craig, Mark Driscoll, Vlad Farcus, Jarrod Faria, Kienan Faria, Michael Gallant, Jamie Gosbee, Joey Greco, Andrew Halliday, Tyrrell Hughes, Rebecca Maxwell, Dylan MacDonald, Mark MacDonald, P hillip MacCallum, Chelsea MacGregor, Lyes Malek, Dave McIver, Iain McPhee, Meghann McPhee, Erin Montelpare, Jennifer Nangreaves, Sam O'Connor, Justin Pater, Michael Rochon, Umesh Roopnarinesingh, Channelle Roy, Sara Russell, Anthony Scott, Amanda Sheppard, Josh Smith, Bridget Vickers, Hannah Waxer, Lauren Wonfor and 朱雪铭 a nd many many others for making such beautiful memories to me.

Table of Contents

List of Tables

List of Figures

Chapter 1: Introduction and Literature Review

1.1 Plant morphology, development and morphogenesis

Plant morphology or the study of plant forms involves looking at regularities, similarities, and analogies under an apparent diversity between individual plants. It reduces this diversity to a few basic categories, opening the way for the analysis of mechanisms and processes related to the generation of forms (Lacroix *et al.*, 2005). In a narrow sense, it only considers the external form of plants. In a wide sense, it considers all levels of organization of plant form (Sattler, 1978).

Plant development can be described as the process by which a single cell (either a fertilized egg or a zygote) grows and develops into an integrated organism while each cell in this multicellular organism acquires and maintains its specialized function (Leyser and Day, 2003).

The process of plant development raises numerous questions for the study of **plant morphogenesis** (Sinnott, 1960). Plant morphogenesis deals with the dynamic and causal aspects of the plant form. The term "morphogenesis" itself means "the origin of form" (Sinnott, 1960). Some have employed this term synonymously with "developmental morphology" (Sinnott, 1960).

One important area in plant development and plant morphogenesis is the investigation of the **shoot apical meristem** (SAM). It is a localized region of tissue which does not undergo tissue differentiation but continually produces the cells which do differentiate (Beck, 2005). The SAM,

which is located at the tip of the shoot apex, functions to produce an expanding shoot system by the continued formation of tissues and the initiation of a succession of leaves in specific configuration. The activity of the SAM results in the production of a continuously growing aerial body of the plant (Steeves and Sussex, 1989).

1.2 Phyllotaxis

During the process of repeated formation of primordia on the SAM, one striking phenomenon that attracts our attention is the enigmatic way the primordia are arranged (Figure 1A). Even when the promordia develop into leaves or floral organs, one can still appreciate the amazing patterns that can be found in nature. Scales on a pine cone (Figure 1B) or on a pineapple, florets on the head of a daisy and seeds in a sunflower are most commonly observed (Adler *et al.*, 1997).

In botany, **phyllotaxis** (phyllotaxy) is devoted to the description, characterization and generation of patterns made by similar building blocks on plants mentioned above and to the study of growth processes leading to their formation (Jean, 1994).

Early studies of phyllotaxis focused on the description of the patterns observed (Bravais and Bravais, 1837) and then the construction and elaboration of different types of models that were designed to explain the origin of phyllotactic patterns (Church, 1904; Hofmeister, 1868; Snow and Snow, 1933; Richards, 1948; van Iterson, 1907). The famous Fibonacci numbers and the Golden Ratio played very important roles in these studies (Adler *et al.*, 1997).

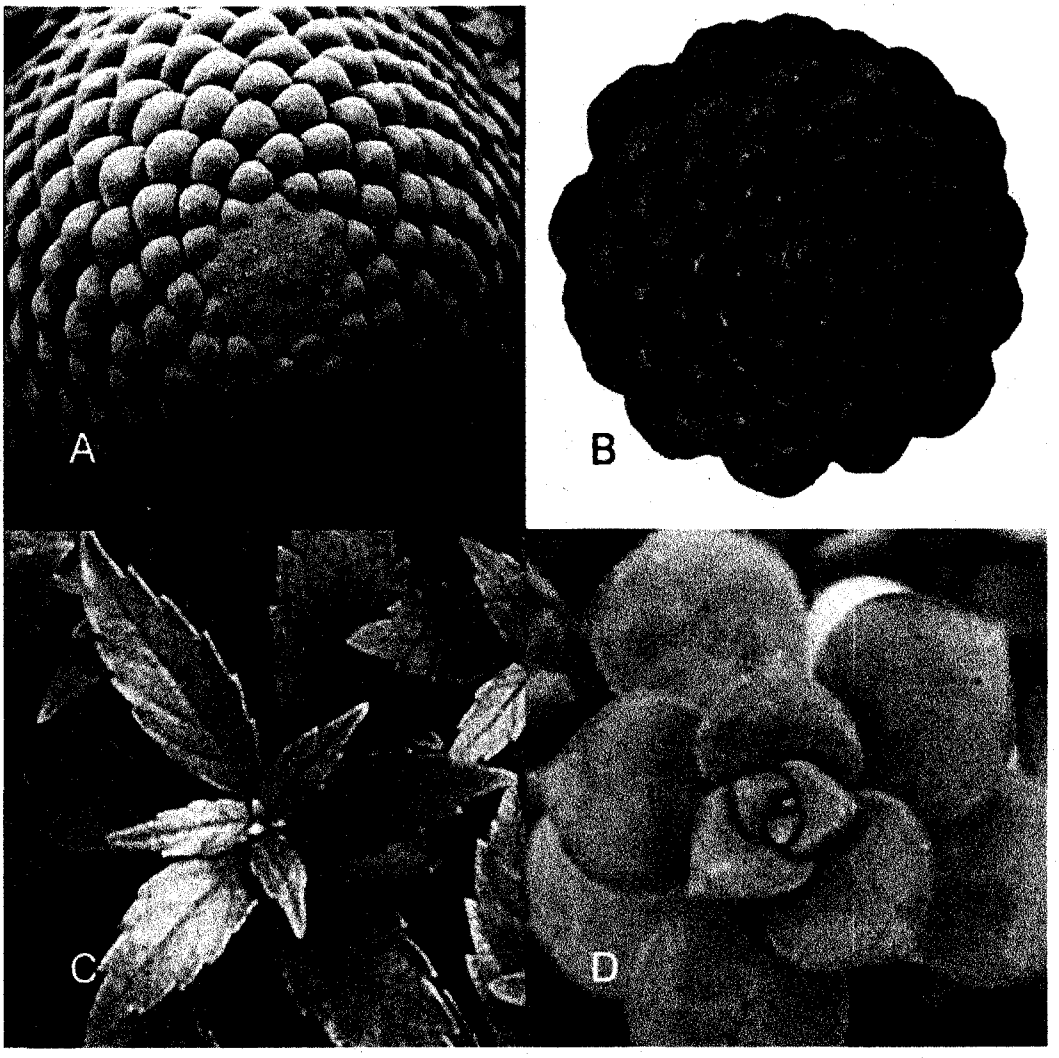

Figure 1: phyllotaxis and phyllotactic patterns. A: primordia on the SAM of a Norway spruce branch (Online image, 6 May 2008. http://www.worldproutassembly.org/archives/2007/08/the_mathematica.html). B: scales on a pine cone (Institute of Systematic Botany, University of Zürich, 2005). C: *Archimenes erecta* shows the whorled pattern (Online image, 6 May 2008. http://maven.smith.edu/~phyllo/About/Classification.html). D: *Aonium* shows the spiral pattern (Online image, 6 May 2008. http://maven.smith.edu/~phyllo/About/Classification.html).

Recent studies of phyllotaxis focused on the mechanisms involved in the formation of phyllotactic patterns (Barabé, 2006). They are studied intensively from the experimental (Berleth *et al.*, 2007; Fleming, 2002, 2005; Fleming *et al.*, 1997; Heisler *et al.*, 2005; Heisler and Jönsson, 2006a; Kuhlemeier and Reinhardt, 2001; Reinhardt, 2005; Reinhardt *et al.*, 2000, 2003, 2005; Reinhardt and Kuhlemeier, 2001; Smith, 2008; Traas and Vernoux, 2002) and the theoretical (Atela *et al.*, 2002; Green, 1999; Hotton *et al.*, 2006; Jean, 1994; Jean and Barabé, 1998a; Levitov, 1991a, 1991b; Meinhardt, 2003, 2004; Newell *et al.*, 2008; Newell and Shipman, 2005; Shipman and Newell, 2004, 2005, 2008) point of views, or both (Douady and Couder, 1992, 1996a, 1996b, 1996c; Jönsson *et al.*, 2006; Smith *et al.*, 2006), or all aspects of phyllotaxis (Jean and Barabé, 1998b).

These works mainly deal with the regular phyllotactic patterns with deterministic models. However, perturbed (chaotic) patterns exist (Barabé, 1991) and can also be found in phyllotactic mutants (Itoh *et al.*, 2000). This phenomenon brings new theoretical problems that cannot be solved by using models designed to analyze regular phyllotactic patterns (Barabé, 2006). A new probabilistic approach to phyllotaxis was thus introduced to study this phenomenon (Barabé, 2006; Barabé and Jeune, 2004; Jeune and Barabé, 2004).

The study of phyllotaxis also involves genetic and molecular approaches (Berleth *et al.*, 2007; Carpenter *et al.*, 1995; Fleming, 2005; Heisler *et al.*, 2005; Heisler and Jönsson, 2006a; Itoh *et al.*, 2000; Jackson and Hake, 1999; Jönsson *et al.*, 2006; Kuhlemeier, 2007; Kuhlemeier and Reinhardt, 2001; Merks *et al.*, 2007; Navarro *et al.*, 2004; Nishimura *et al.*, 2002; Otsuga *et al.*, 2001;

Reinhardt, 2005; Reinhardt *et al.*, 1998, 2000, 2003; Smith, 2008; Takahashi *et al.*, 2002; Tamaoki *et al.*, 1999; Veit *et al.*, 1998) as well as computer simulations (de Reuille *et al.*, 2006; Heisler and Jönsson, 2006b; Hellwig *et al.*, 2006; Kramer, 2008; Prusinkiewicz and Rolland-Lagan, 2006; Smith *et al.*, 2006).

1.3 Descriptive aspects of phyllotaxis and some basic concepts

The phyllotaxis of any one plant, or at least any one shoot of a plant, is usually of diagnostic value to identify a plant (Bell, 1991). Moreover, phyllotaxis plays an important role in determining the branching pattern of a plant (Bell, 1991). The study of phyllotaxis encompasses the symmetrical constructions determined by leaves or floral organs, their origins, their functions and also their interactions with the environment (Jean, 1995). A specific construction formed by primordia, organs or parts of organs is called a **phyllotactic pattern** (system) (Jean, 1994).

The building blocks of the phyllotactic pattern, either primordia or mature organs, differ in number, size, position, shape and rate of formation, etc., thus giving considerable diversity to the formation of phyllotactic patterns (Jean, 1995). However, in general, most of the phyllotactic patterns can be grouped into two large categories: **whorled pattern** (Figure 1C) and **spiral pattern** (Figure 1D) (Jean, 1994).

The whorled pattern has a specific number (n) of primordia inserted at the same level of the shoot apex or organs at the same node on the stem (Jean, 1994). N can sometimes be as big as 20 and

varies from species to species, or even in the same specimen (Jean, 1994). In a whorled pattern, it is easy to observe vertical lines of primordia or organs and theses lines are parallel to the axis of the shoot apex or the stem. Each of these lines is called an **orthostichy** (Jean, 1994).

When the primordia or organs in each whorl are directly above those of the preceding whorl, the pattern is called **superposed** (Jean, 1994). The number of orthostichies in a superposed whorled pattern is equal to n. When the primordia or organs in each whorl are located in the gaps of the ones in the preceding whorl, the pattern is called **alternating** (Jean, 1994). The number of orthostichies in an alternating whorled pattern is equal to $2n$.

For the alternating whorled patterns, when $n = 1$, it is called **distichous**; when $n = 2$, it is called **decussate**; when $n = 3$, it is called **tricussate** (trimerous); and so on (Jean, 1994). Barabé (2006) categorizes the distichous pattern as a third category of phyllotactic pattern along with whorled and spiral patterns.

The spiral pattern is the most common phyllotactic pattern in nature (Jean, 1994). It also has a specific number of J (most commonly $J = 1$) primordia inserted at the same level of the shoot apex or organs at the same node on the stem (Jean, 1994). But differently from the whorled pattern, it is possible to observe two (or more) families of spirals around the shoot apex or the stem which curve in different directions and appear to cross one another. These spirals are called **parastichies** (Figure 2A) (Jean, 1994).

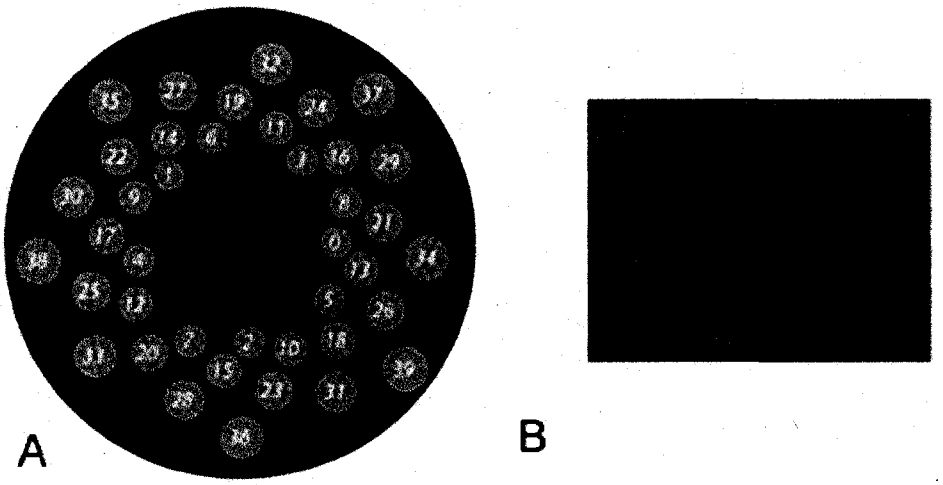

Figure 2: A: centric presentation of a spiral pattern. The numbers are from the youngest primordium to the oldest. Each curve drawn is a parastichy. Each counter clockwise curve belongs to an 8-parastichy whereas each clockwise curve belongs to a 13-parastichy. All the 8-parastichies constitute a family of parastichies and all the 13-parastichies constitute another family of parastichies and these 2 families of parastichies constitute a parastichy pair. (8, 13) is the secondary number of this parastichy pair. If we consider each little circle as a primordium, the parastichies are called contact parastichies and a parastichy pair becomes a contact parastichy pair. If we consider each little circle as the center of a primordium, the parastichies are called visible opposed parastichies and a parastichy pair becomes a visible opposed parastichy pair. A visible opposed parastichy pair becomes the conspicuous parastichy pair when the angle of intersection of parastichies is the closest to 90°. (8, 13) is the conspicuous parastichy pair because its angle of intersection of parastichies is the closest to 90° among others, which are not presented here. Therefore, the pattern is (8, 13) (Online image, 6 May 2008. http://maven.smith.edu/~phyllo/About/Lattices/SpiralLattices.html). B: cylindrical presentation of a spiral pattern. The numbers are from the youngest primordium to the oldest. Each dot is a primordium (Online image, 6 May 2008. http://www.swintons.net/deodands/archives/cat_glossary.html).

A parastichy in a family containing n parastichies is called an ***n*-parastichy** (Figure 2A) (Jean, 1994). The parastichies running in the same direction constitute a **family of parastichies** (Figure 2A) (Jean, 1994). Two families of parastichies running in different directions constitute a **parastichy pair** (Figure 2A) (Jean, 1994). A parastichy pair formed by a family of m parastichies in one direction and a family of n parastichies in another direction is denoted (m, n). The numbers m and n are called the **secondary numbers of the parastichy pair** (Figure 2A) (Jean, 1994).

When the sides of the primordia are in contact, the parastichies are easy to observe and are called **contact parastichies** (Figure 2A) (Jean, 1994). The parastichies running in the same direction constitute a **family of contact parastichies** (Jean, 1994). Two families of contact parastichies running in different directions constitute a **contact parastichy pair** (Figure 2A) (Jean, 1994).

Relative to the contact parastichy and contact parastichy pair, the **visible opposed parastichies** and **visible opposed parastichy pair** is defined from another point of view in which each primordium is represented as a dot at its geometrical center. In this case at each intersection of two visible opposed parastichies there is a dot (primordium) present (Figure 2A) (Jean, 1994). A visible opposed parastichy pair may or may not be a contact parastichy pair (Rutishauser, 1998). In one pattern, there could be more than one visible opposed parastichy pair, but there is generally only one **conspicuous parastichy pair** (Figure 2A) (Jean, 1994). Among all the visible opposed parastichy pairs, the conspicuous parastichy pair has an **angle of intersection of parastichies** (γ) (Figure 2A) closest to 90° (Jean, 1994). When a pattern shows the conspicuous parastichy pair (m, n), we say that the **phyllotaxis of the pattern** is (m, n) (Figure 2A) (Jean, 1994).

The **genetic spiral** is a continuous hypothetical curve going through the consecutively borne primordia from the oldest to the youngest by the shortest path around the center (Jean, 1994). The number of genetic spirals in a spiral pattern is equal to J; the number of genetic spirals in a whorled pattern is equal to n.

In nature, in more than 90% of the cases the secondary numbers of a pattern (m, n) are consecutive terms in the **Fibonacci sequence** (1, 1, 2, 3, 5, 8, 13, 21, ...,) (Jean, 1994). The Fibonacci sequence is formed by a simple addition rule:

$$F_{k+1} = F_k + F_{k-1}$$

Where $k = 2, 3, 4, \ldots$, and $F_1 = F_2 = 1$. Closely related to the Fibonacci sequence is the **Golden Ratio** (φ). It is the limit of the ratios of successive terms of the Fibonacci sequence ($\varphi \approx 1.618$). These patterns are called Fibonacci patterns (Jean, 1994). Other patterns observed in nature are based on similar sequences. For example, Lucas pattern (first accessory pattern) is based on the sequence (1, 3, 4, 7, 11, 18, 29, 47, ...,).

One diagrammatic method to study the phyllotactic pattern is to cut the shoot apex at right angles to its axis and draw the positions of primordia (or their centers). This is known as the **centric representation** (disc representation) (Figure 2A) (Church, 1904; Richards, 1948). Ideally, each family of parastichies is a set of identical and evenly spaced logarithmic spirals with the center of the SAM as their collective pole (Jean, 1994). One disadvantage of the centric representation is that it does not take into account the three-dimensional aspect of the growing shoot apex. However, it is still very useful in empirical studies, especially for calculating the phyllotactic parameters on

optical microscope slides (Adler *et al.*, 1997).

The other diagrammatic representation to study phyllotactic patterns (especially spiral patterns) is to consider the primordia (or their centers) as points on the surface of a cylinder. This is known as the **cylindrical representation** (Figure 2B) (Bravais and Bravais, 1837). Each family of parastichies is a set of identical and evenly spaced helices running upwards around the cylinder. When the cylinder is unfolded into a plane by cutting its surface along a vertical line which goes through the youngest primordium, the helices become straight lines and the primordia on the lines form a lattice (Jean, 1994). It is important to note that the centric and the cylindrical representations are mathematically equivalent. The centric representation can be obtained from the cylindrical representation by using a logarithmic transformation or an exponential transformation and *vice versa* (Adler *et al.*, 1997).

In general, phyllotactic patterns can be accurately described by using 4 parameters among others: divergence angle (d), plastochrone ratio (R), conspicuous parastichy pair (m, n) and their angle of intersection (γ) (Barabé, 2006).

Divergence angle (d) is defined as the smaller of the two angles determined by two successive primordia measured from the center of the shoot apex (Figure 3). In addition, another measure related to phyllotaxis involves the plastochrone. Although plastochrone is the time interval between the initiations of two successive primordia, **Plastochrone ratio** (R) is defined as the ratio of distances of two successive primordia measured from the center of the shoot apex (Figure 3).

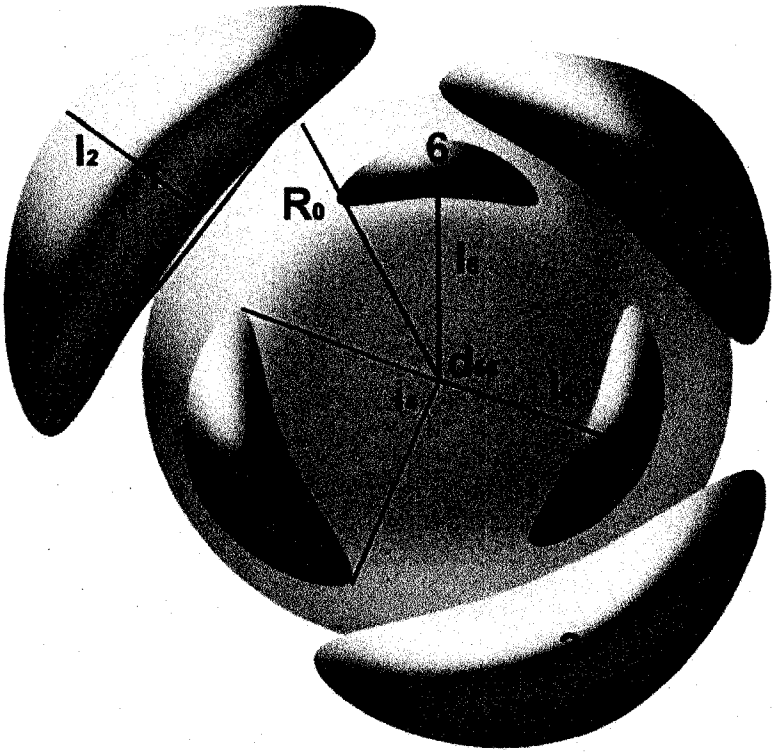

Figure 3: phyllotactic parameters. d_{56}: divergence angle (d) between primordia 5 and 6; l_5 and l_6: distances from the center of the SAM to the center of primordia 5 and 6, respectively, plastochrone ratio (R) is calculated as: $R_{56} = l_6/l_5$; i_4: leaf insertion angle (i) of primordium 4; R_0: the radius of the SAM; l_1 and l_2: tangential and radial lengths of a primordium, respectively, parameter Γ is calculated as: $\Gamma = l_1/R_0$ (Modified from Barabé, *et al.* (2007)).

In order to link these 4 parameters (d, R, (m, n) and γ) together theoretically, Richards (1948, 1951) proposed the concept of "Phyllotaxis Index" (P.I.) and it is defined as:

$$\text{P.I.} = 0.3791 - 2.3925\log_{10}(\log_{10}(R))$$

The phyllotaxis Index will be represented by integers (e.g., 1, 2, 3 and so on) when γ of a Fibonacci pattern is 90°. For the ideal Fibonacci patterns (d is equal to 137.5°) and the real Fibonacci patterns (d between 120° and 180°), the relations between d, R, (m, n) and γ were highlighted by Richards (1951). For example, when γ of an ideal (3, 5) Fibonacci pattern is 90°, P.I. is equal to 3, and thus R can be calculated and its value is 1.20. Theoretically, for the ideal Fibonacci patterns, as (m, n) increases, P.I. also increases whereas R decreases.

Jean (1994) proposed a dynamical model:

$$r = (m+n)^{-2}\varphi^3(\sqrt{5}\cot\gamma + \sqrt{(5\cot^2\gamma + 4)})/2\sqrt{5}$$

where r is the radial spacing between two successive primordia in the cylindrical representation and it is calculated as:

$$r = \ln(R)/2\pi)$$

and φ is the Golden Ratio. This model and other equations known as accessorial propositions derived from this model link these 4 parameters (d, R, (m, n) and γ) together and allow phyllotactic patterns to be recognized easily, accurately and efficiently. For all the combinations of these parameters, knowing some of them make it possible to deduct others from the Pattern Determination Table derived from this model (Jean, 1994). This model is more favored than the Phyllotaxis Index, because it considers all possible spiral patterns and the angles of intersection of the visible opposed parastichy pair, whether orthogonal or not (Jean, 1995).

The size of the SAM and the size of the primordia are important features that determine the phyllotactic pattern. Van Iterson (1907) defined the parameter b as:

$$b = d_0/2\pi R_0$$

where d_0 is the diameter of the primordium and R_0 is the radius of the SAM. Douady and Couder (1996b) defined a similar parameter Γ (Figure 3) as:

$$\Gamma = d_0/R_0$$

It can be calculated as:

$$\Gamma = \sqrt{(l_1 l_2)}/R_0$$

where l_1 is the tangential length of a primordium and l_2 is the radial length of a primordium and it can be approximated as:

$$\Gamma = l_1/R_0$$

Plastochrone ratio (R) can be also used for the same purpose by using the area ratio A (Richards, 1951). It is defined as the ratio of the mean area of the SAM to the area of the primordium at initiation and it can be calculated as:

$$A = 1/(2\ln(R))$$

In addition to the theoretical study of the phyllotactic parameters, there are also empirical relationships between them. The empirical relationships include 4 parameters: divergence angle (d), plastochrone ratio (R), contact parastichies (cp) and leaf insertion angle (i) (Rutishauser, 1998).

Leaf insertion angle (i) is defined as the angle determined by the coverage sector of a primordium measured from the center of the SAM (Figure 3) (Rutishauser, 1998).

Rutishauser (1998) studied 170 shoot apices of different species of vascular plants (ferns, gymnosperms, flowering plants, mainly eudicotyledons) and established empirical relationships of different phyllotactic patterns. He concluded that each phyllotactic pattern is characterized by certain ranges of values with respect to these parameters and a limit value for the divergence angle (Rutishauser, 1998). For example: Fibonacci patterns are correlated with very large amplitudes for R (1.001 ~ 1.67) and i (4.5° ~ 360°), whereas Lucas patterns have more clearly defined limits for R (1.036 ~ 1.24) and i (35° ~ 79°).

All the parameters mentioned above are based on the centric representation, which is two-dimensional. However, shoot apices are usually domed (Williams, 1975). So far, the only parameter concerning the three-dimensional shape of the shoot apex is the apical angle of the SAM (ψ) (van Iterson, 1907; Richards, 1951). It can be calculated as:

$$\psi = 2\arcsin(l_2/l_1)$$

where l_1 is the tangential length of a primordium and l_2 is the radial length of a primordium (Douady and Couder, 1996b).

In order to study the actual three-dimensional shape of the shoot apex, some new parameters need to be introduced: volume of the SAM (v), surface area of the SAM (the actual three-dimensional area of the SAM) (sa), projected area of the SAM (the cross sectional of the SAM) (pa) and height of the SAM (h).

1.4 Hypotheses and models of phyllotaxis

The investigation of phyllotactic patterns, especially the multiplicity of parastichies, has puzzled scientists for years (Jean, 1995). In addition to the descriptive aspects of phyllotaxis, there are more fundamental matters as far as underlying causes of phyllotactic patterns are concerned. This leads to some deeper questions. How do plants achieve such precise pattern formation? Where does the control come from to establish the pattern? To answer these questions, it is necessary to build mathematical models based on botanical hypotheses. The main previously proposed hypotheses and/or models can be categorized into three groups: physical, chemical and global (Jean, 1994).

Physical hypotheses emphasize the mutual physical contact between the "biological entities", e.g., between primordia and the SAM or only between the primordia. Hofmeister (1868) suggested that new primordia at the SAM arise periodically at regular time intervals at the largest possible gap between the existing primordia. This hypothesis was later called "Hofmeister axiom" and has had a great influence on studies that followed.

Hofmeister's idea was modified by Snow and Snow (1931, 1933). They conducted experiments on *Lupinus albus* and showed that the position of the new primordium depends on the positions and shapes of previous primordia. In addition, if the position of the gap of the previous primordium is altered, the position of the new primordium is also altered accordingly. These results were later interpreted as the "first available space" theory (Snow and Snow, 1952, 1962).

Physical hypotheses infer mechanical pressure as a way by which primordia are produced (Newell *et al.*, 2008). Adler (1974, 1977) proposed the contact pressure model which is based on two assumptions: (1) there is a time period during which the girth of the plant grows faster than the internode distance of the plant; (2) there is a time period during which the minimum distance between primordia is maximized. He showed that if these two time periods are overlapping, then the divergence angle oscillates alternately decreasing and increasing with smaller and smaller ranges and converges to a limit. He also showed that if the time period that maximizes the minimum distance between primordia begins early; this divergence angle limit is the golden angle, which means the manifestation of the Fibonacci pattern is inevitable. This model puts order into the seemingly confusing multiplicity of parastichies and divergence angles observed on plants together in various mathematical ways (Adler *et al.*, 1997).

The work of Levitov (1991a, 1991b) on the positioning of vortices in superconducting lattices and the work of Douady and Couder (1992, 1996a, 1996b) on producing phyllotactic patterns by using droplets of ferrofluid in a magnetic field, pointed to the idea that phyllotactic patterns minimize a certain type of free energy (Newell *et al.*, 2008).

Green (1999) suggested that differential growth between the tunica and the corpus generates compressive stresses and leads to buckling on the surface of the SAM. Dumais and Steele (2000) showed these compressive stresses on sunflowers. Green's model was primarily a linear mathematical model, suggesting how a buckled surface begins. However, the actual buckling manifested by the plant is determined by non-linear mathematical models, which were ignored

(Newell *et al.*, 2008). Shipman and Newell (2004, 2005) emphasized two new features, quadratic coupling and bias, which play central roles in the non-linear mathematical models and also showed how they play an important role in favoring Fibonacci patterns over alternative patterns.

Chemical hypotheses (reaction-diffusion) interpret the origin of the phyllotactic patterns as diffusion fields of chemical inhibitor or activator, such as auxin, released fr om the existing primordia and/or the SAM. A primordium arises when the concentration of the inhibitor or activator is below or above a threshold (Jean, 1994). Schoute (1913) proposed that the initial placement of primordia is determined by a chemical inhibitor secreted by the existing primordia to prevent a new primordium from being initiated too close. Schoute's hypothesis was favored by Richards (1948) and Wardlaw (1949).

Turing (1952) suggested that a system of chemicals, called morphogens, reacting together and diffusing through tissue is responsible for the phenomenon of morphogenesis. His investigation of this reaction-diffusion system on an isolated ring of cells was chiefly concerned with the onset of instability of the homogeneous equilibrium which accounts for the phenomenon of phyllotaxis in two-dimensions.

Schwabe and Clewer (1984) developed a model based on auxin inhibitors. Veen and Lindenmayer (1977) and Meinhardt (1984) included both activator and inhibitor in their models. Recently, Berleth *et al.* (2007), Heisler *et al.* (2005), Heisler and Jönsson (2006a), Jönsson *et al.* (2006), Kuhlemeier (2007), Kuhlemeier and Reinhardt (2001), Merks *et al.* (2007), Reinhardt (2005), Reinhardt *et al.* (2000, 2003) and Smith *et al.* (2006) indicated that auxin and its interaction with

the PIN1 transport protein plays a very important role in the initiation of primordia.

It is important to be aware that physical and chemical hypotheses are complementary rather than contradictory. Newell *et al.* (2008) showed that these two groups of hypotheses' models' partial differential equations are similar in form. A combined model that incorporates the coupling of physical factors and chemical factors was developed by Newell *et al.* (2008). This model can be analyzed by using a set of ordinary differential equations and can thus reveal the parameter choices under which the two mechanisms may cooperate to determine the pattern, or under which one or the other mechanism may dominate (Newell *et al.*, 2008).

Jean (1994) proposed a **global hypothesis** of phyllotaxis. This hypothesis includes an interpretative model where the growth of leaf distribution is viewed as a succession of cycles (hierarchies). Each cycle extends the preceding one by adding new leaves. The cycles are then joined to each other to form a reversed tree-like diagram with single and double nodes only. This diagram is called a hierarchy. An entropy-like function can then be defined on the set of hierarchies representing the various phyllotactic patterns and by using a principle of optimal design, the cost of each pattern can be calculated. This model suggested that the Fibonacci pattern has the minimum cost and other spiral patterns can be acquired by adding that cost (Jean, 1994).

1.5 Transition of phyllotactic patterns

During the growth processes of some plants, the phyllotactic pattern of the SAM will change. This

is called **transition** (Zagórska-Marek, 1987). It can be also viewed as a symmetry-breaking process of the previous pattern (Yamada *et al.*, 2004). Two types of transitions have been postulated to occur in nature: continuous and discontinuous (Zagórska-Marek, 1987). Whether the SAM has the ability for continuous transition or discontinuous transition depends mainly on its genetics (Rutishauser, 1998).

Continuous transition occurs via symmetrical expansions or contractions of the circumference of the stem, resulting in uniform changes in the global relationships between the primordia (Meicenheimer and Zagórska-Marek, 1989). It leads to changes in phyllotaxis from (m, n) to $(m + n, n)$ or from (m, n) to $(m, n - m)$ $(m < n)$ (Jean and Barabé, 2001). Pattern transitions from a (5, 8) spiral pattern to a (8, 13) spiral pattern as seen in *Linum usitatissimum* and from a (8, 13) spiral pattern to a (13, 21) spiral pattern as seen in *Picea abies* are examples of continuous transitions (Rutishauser, 1998).

A continuous transition cannot reverse the chirality of the genetic spiral (Meicenheimer, 1998). However, it can lead to a decrease in plastochrone ratio (R) and leaf insertion angle (i) (Rutishauser, 1998). Continuous transitions have been observed in nature (Erickson and Meicenheimer, 1977; Meicenheimer, 1979, 1982, 1987; Williams, 1975) and can also be chemically induced (Maksymowych and Erickson, 1977; Schwabe, 1971).

Discontinuous transition occurs via asymmetrical expansions or contractions in localized sectors of the circumference of the stem, resulting in additional or fewer primordia inserted or deleted

from the previous pattern (Meicenheimer and Zagórska-Marek, 1989). It leads to changes in phyllotaxis from (m, n) to (m, n - 1) or from (m, n) to (m - 1, n) ($m > n$) (Jean and Barabé, 2001). Pattern transitions from a decussate pattern to a Fibonacci pattern as seen in *Picea abies* and from a Fibonacci pattern to various accessory patterns as seen in *Anagallis arvensis* and *Bryophyllum tubiflorum* are examples of discontinuous transitions (Rutishauser, 1998).

A discontinuous transition may reverse the chirality of the genetic spiral (Meicenheimer, 1998). It can even involve a change from a regular phyllotactic pattern to a perturbed (chaotic) pattern, especially when the plastochrone ratio (R) and leaf insertion angle (i) are very low ($R < 1.02$, $i <$ 45°) and/or when a large number of primordia are rapidly initiated, such as in *Acacia* (Rutishauser, 1986). Discontinuous transitions have been observed in nature (Meicenheimer, 1979, 1982, 1987; Zagórska-Marek, 1985, 1987, 1994) and can be surgically (Snow and Snow, 1935) and chemically (Meicenheimer, 1981; Snow and Snow 1937) induced. Recently, by using a new approach based on the group theory, Yamada *et al.* (2004) were able to produce discontinuous transitions from other patterns theoretically.

The most prevalent discontinuous transition in eudicotyledon families is the transition from the decussate pattern to the spiral patterns (Meicenheimer, 1998). Hutchinson (1973) investigated 320 eudicotyledon families and indicated that 47 (14.7%) families are characterized exclusively by decussate (or whorled) patterns whereas 162 (50.6%) families are characterized exclusively by spiral patterns and with the remaining 111 (34.7%) families have both decussate and spiral patterns. This indicates that over half of all the eudicotyledon families undergo a discontinuous

transition from the decussate pattern to the spiral patterns early during the development of the seedling because all the eudicotyledonous shoot systems begin with two oppositely arranged cotyledons. In addition, many eudicotyledon families undergo a discontinuous transition from the decussate pattern to the spiral patterns during the reproductive transformation of the SAM (Meicenheimer, 1998). Therefore, the discontinuous transition from the decussate pattern to the spiral patterns is the most common among dicotyledons (Meicenheimer, 1998).

The phyllotaxic triangular unit (PTU) was proposed (Zagórska-Marek, 1987) and advanced (Meicenheimer and Zagórska-Marek, 1989; Zagórska-Marek, 1994, 2003) to study discontinuous transitions. It is defined by triads of primordia located on contact parastichies. The primordium at a higher position is the vertex of the triangle with two other adjacent primordia located on two different contact parastichies (or the conspicuous parastichiy pair (Jean, 1994)) at lower positions are the two other points of the triangle. The PTU represents the smallest common element for all patterns. The PTUs are postulated to repeat themselves by the iterative principle that two upper primordia of adjacent PTUs form the base of the next PTU (Zagórska-Marek, 1987).

To use the PTU concept to explain the discontinuous transition, it is postulated that additional or fewer PTUs may be inserted or deleted from the previous pattern by making reference to a system which involves adding or deleting bubbles in bubble raft crystals (Harris, 1977, 1978; Ishida and Iyama, 1976) floating on the surface on the water (Zagórska-Marek, 1987). However, the empirical study in *Linum usitatissimum* and *Epilobium hirsutum* indicates that the PTU is inadequate to provide a mechanism for the discontinuous transition (Meicenheimer, 1998).

Discontinuous transitions are much less frequent than continuous transitions and are more enigmatic (Jean and Barabé, 1998a). They raise numerous morphological and theoretical questions, especially in the context of transitions from the decussate pattern to the spiral patterns (Adler *et al.*, 1997). Although discontinuous transitions have been studied from descriptive (Guédès and Dupuy, 1983; Meicenheimer, 1979, 1981, 1982, 1987, 1998; Rutishauser, 1998; Zagórska-Marek, 1985, 1987, 1994), experimental (Meicenheimer, 1979, 1981, 1982, 1987, 1998; Snow and Snow, 1935, 1937) and theoretical (Douady and Couder, 1996c; Jean, 1994; Jean and Barabé, 2001; Meicenheimer and Zagórska-Marek, 1989; Yamada *et al.*, 2004; Zagórska-Marek, 1985, 1987, 1994; Zagórska-Marek and Szpak, 2008; Zagórska-Marek and Wiss, 2003) points of view, they have not been fully incorporated within theoretical models yet and a lot of questions still remain unanswered, such as how to create new models that are able to predict and simulate discontinuous transitions that naturally occur (Meicenheimer, 1998).

To further advance our knowledge of discontinuous transition, the seedling of *Thuja occidentalis*, which presents different phyllotactic patterns, may be a good material to study particular discontinuous transitions.

1.6 Pattern transition in *Thuja occidentalis*

Thuja occidentalis (eastern white cedar) is a gymnosperm that belongs to the family *Cupressaceae*. Also known as Eastern arborvitae, American arborvitae and northern white cedar, *T. occidemtalis* is one of the two cedar species that are native to North America (Nour *et al.*, 1993). It is important

in both forestry and horticulture (Nour *et al.*, 1993).

The architectural organization of mature *T. occidentalis* has six orders of vegetative axes and is highly complex (Briand *et al.*, 1991). Its branching is "sylleptic, diffuse and with usually one branch at each node in first-order to fifth-order branch", while sixth-order branch does not branch (Briand *et al.*, 1991). The leaves on first-order branch are "imbricate and scale-like with stiffly spread acuminate apices" while leaves on second-order branch are also "imbricate and scale-like but with closely appressed to stiffly spread apices ranging from acuminate to acute". From third-order to sixth-order branch, marked leaf dimorphism: facial and lateral is easily distinguishable. The facial leaves are "scale-like, flattened and closely appressed to the stem and have acute to obtuse apices". The lateral leaves are "scale-like, folded along their midline, closely appressed to the stem and have acuminate to acute or rarely obtuse apices" (Briand *et al.*, 1991).

This dimorphism on the side branches is even marked at the level of the SAM where leaves in one plane are wide and flat (corresponding to the facial ones on mature plants) whereas leaves in a plane perpendicular to the previous pair are narrower and cup-shaped (corresponding to the lateral ones on mature plants) (Lacroix *et al.*, 2004). When the leaf primordia are initiated, either type is initiated in pairs at the same time and opposite to each other. The initiation of the primordia of either type can be generally divided into three developmental stages. In stage one, the initiation of the new pair of primordia begins to take place when the previous pair of primordia covers the SAM. In stage two, both types of leaves are similar in appearance as buttresses and gradually gain the characteristics of each type. In stage three, a distinct furrow is noticeable between each

primordium and the SAM (Lacroix *et al.*, 2004). Even though both types of leaves are similar when they are initiated, visible morphological differences are discernable after just one plastochrone, i.e., before the next pair of leaves is initiated. This cycling process results in the fluctuation in the size of the SAM (Lacroix *et al.*, 2004).

It was observed that the shoot of *T. occidentalis* after germination is bilateral in symmetry (Nour *et al.*, 2004) and later on produces spirally arranged leaves (Lacroix *et al.*, 2004). However, on side branches, a decussate pattern is observed (Briand *et al.*, 1991; Lacroix *et al.*, 2004). At first glance, these appear to be representative of discontinuous transitions. When does this transition happen? Which parameters change to affect these transitions? The details and mechanisms involved are unknown. To answer these questions, a quantitative analysis of different phyllotactic parameters for each pattern has to be done at the level of the SAM.

1.7 Objectives

(1) To describe the general architecture of seedlings of *T. occidentalis* to visualize the pattern transition and leaf shape changes that take place in different axis orders.

(2) To establish the mathematical basis of each phyllotactic pattern in seedlings of *T. occidentalis*. The phyllotactic parameters to be measured and calculated of each phyllotactic pattern using optical microscopy (OM) include: divergence angle (d), plastochrone ratio (R), leaf insertion angle (i), parameter Γ and apical angle of the SAM (ψ). The phyllotactic parameters to be measured for

each phyllotactic pattern using the scanning electron microscopy (SEM) include: volume of the SAM (v), surface area of the SAM (the actual three-dimensional area of the SAM) (sa), projected area of the SAM (the cross sectional of the SAM) (pa) and height of the SAM (h). These data can eventually validate the empirical relationships between phyllotactic parameters and improve theoretical predictive models of phyllotaxis.

(3) To document the pattern transition in seedlings of *T. occidentalis* to provide new insights into our understanding of discontinuous transition in plants.

Chapter 2: Material and Methods

2.1 Specimen collection

Seedlings of *T. occidentalis* were obtained from the Frank J. Gaudet tree nursery, Charlottetown, PE, Canada. Plantlets less than one year old were used for the characterization of the phyllotactic pattern. The root system of each seedling was cut and the aerial part was fixed in the FAA (38% formaldehyde: glacial acetic acid: 70% ethanol = 1:1:18 by volume) solution for at least 24h prior to dissection.

2.2 Specimen dissection

Fixed *T. occidentalis* shoots were dissected in 70% ethanol. The leaves were removed from the oldest to the youngest and their positions were recorded for the general architecture until the shoot apex was exposed. The branches and the sequence of leaves on the branches were also described. Leaves on shoots used for the optical microscopy (OM) study were removed until about 10 were leaves left for the spiral pattern and 5 to 6 whorls were left for the whorled patterns. Each shoot was embedded in a small piece of pith tissue in order to keep the shoot apex at right angle to the plane of sectioning. Leaves on shoots used for the scanning electron microscopy (SEM) were removed sequentially until the SAM and its leaf primordia were exposed.

2.3 Optical microscopy (OM)

Twenty shoot apices from the main stem of the seedlings of *T. occidentalis* and 10 shoot apices from the side branches (second-order and third-order) of the seedlings of *T. occidentalis* were fixed and dissected as indicated previously and eventually dehydrated in a graded tertiary butyl alcohol (TBA) series (Appendix A). Prior to paraffin embedding, shoot apices were transferred to a 1:1 mixture of pure TBA and molten paraffin at 61C for 12h, followed by 2 changes of molten paraffin at 61C for 12h each. Each shoot sample was oriented and embedded in a fresh paraffin mold with its shoot apex at right angle to the plane of sectioning. Each mold was then filled with molten paraffin and placed on crushed ice for hardening. Unused blocks were stored at 4C in a refrigerator. An American Optical (AO) Spencer 820 rotary microtome was used to section each block and section thickness was set at 9μm. Prior to mounting the ribbons, a clean slide was smeared with a mixture of 2 drops of Haupt's adhesive (Appendix B) and 5 drops of 4% Formalin. Ribbons were cut to an appropriate length for a slide and mounted on top of the mixture. Each slide was then placed on a warming table set at approximately 60C until the paraffin turned translucent without melting. This provides maximum stretching of the ribbons on the slide. Slides were stained using toluidine blue (TB) according to a standard protocol (Appendix C).

2.4 Scanning electron microscopy (SEM)

Fifty-one shoot apices from the main stem of the seedlings of *T. occidentalis* at different stages of development and 47 shoot apices from the side branches (second-order and third-order) of the

seedlings of *T. occidentalis* were dried in a LADD model 28000 critical point drier using CO_2 as the transitional fluid, mounted on metal stubs, grounded with conductive silver and sputter coated with gold-palladium to approximately 30nm using a Denton Vacuum Desk II sputter coater. The shoot apices were viewed with a Cambridge Instruments S-604 SEM with a digital imaging program SEMICAPS®. A series of 3 micrographs were taken for each shoot sample to take measurements of three-dimensional features (see next section). The first one was taken from the top most view (0° view). Then the platform of the specimen holder of the SEM was tilted 5° in one direction (+5° view) and 5° in the opposite direction (-5° view) in relation to the 0° point of reference. The orientation of the platform was adjusted slightly each time to keep the position of the shoot apex in the same frame of reference as its original position.

2.5 Measurement and calculation of phyllotactic parameters

For OM, each slide was examined under an Olympus BH-2 stereo microscope. Images of each shoot sample were taken using a Leica DC480 digital camera with the Leica® imaging program Image Manager 50. Each image was pre-processed using Adobe Photoshop 7.0® to label the center of the SAM and each primordium. The center of the SAM was determined by rings of cells. The center of each primordium was determined by the central vascular bundle. Phyllotactic parameters were either measured by the Leica® imaging program Image Manager 50 or calculated.

The divergence angle (*d*) was measured directly by using the centers of two successive primordia and the center of the SAM (see Figure 3). The leaf insertion angle (*i*) was measured directly by

using the two widest points on the primordium and the center of the SAM (see Figure 3). The mean value of i for each shoot sample was calculated as the mean value of i for the first 3 leaves.

To calculate plastochrone ratio (R), the distances of two successive primordia were measured first from the center of the SAM to the centers of the primordia and then the older primordium's distance was divided by the younger primordium's distance (see Figure 3). To calculate the mean plastochrone ratio (Rm), the methods described by Rutishauser (1998) were used. For a spiral pattern, it is calculated as:

$$Rm = (Ry/Rx)^{1/(y-x)}$$

where Rx and Ry are the distances from the center of the SAM to the centers of the youngest and the oldest primordium, respectively, and $(y\text{-}x)$ is the plastochrone difference between the youngest and the oldest primordium. For a whorled pattern, it is calculated as:

$$Rm = (Ry/Rx)^{1/n(y-x)}$$

where Rx and Ry are the average distances from the center of the SAM to the centers of the primordia of the youngest and the oldest whorl, respectively, n is the number of primordia per whorl and $(y - x)$ is the plastochrone difference between the youngest and the oldest whorl.

To calculate parameter Γ and apical angle of the SAM (ψ), the methods described by Douady and Couder (1996b) were used. The maximum and the minimum radius of the SAM were measured as R_{max} and R_{min} and their average was calculated as the radius of the SAM (R_0). A line was drawn from the center of the SAM to the outer edge of the primordium passing through its center point. The part of this line that was in the youngest primordium was measured as l_2. Another line at right

angle to the first line was then drawn passing through the center of the primordium. The part of the second line that was in the youngest primordium was measured as l_1. Parameter Γ was calculated as:

$$\Gamma = l_1/R_0$$

Parameter Γ was also calculated as:

$$\Gamma = \sqrt{(l_1 l_2)}/R_0$$

and

$$\Gamma = 2\sin(i_1/2)$$

in order to compare methods. The apical angle of the SAM (ψ) was calculated as:

$$\psi = 2\arcsin(l_2/l_1)$$

For SEM, each series of 3 micrographs was pre-processed using Adobe Photoshop 7.0®. The size of each micrograph was first adjusted to a ratio of 3:4. Each micrograph was then rotated 90° counter-clockwise. The +5° view and the -5° view were identified as left 5° view and right 5° view, respectively. Each series of the pre-processed micrographs was further processed using the 3D reconstruction software MeX® 5.0.1. A digital evaluation model (DEM) was constructed by the program. The following phyllotactic parameters were then measured for each DEM: volume of the SAM (*v*), surface area of the SAM (*sa*), projected area of the SAM (*pa*) and height of the SAM (*h*).

2.6 Statistical tests used

All statistical tests were done using Minitab® 15.1.0.0 software (Minitab Inc., 2006). A two-sample *t*-test was used to compare if two groups of data were significantly different. A two-sample paired *t*-test was used to compare if two groups of paired data were significantly different. One-way analysis of variance (one-way ANOVA) was used to compare if more than two groups of data were significantly different. Tukey's multiple-comparisons was used (as necessary) to determine which two (or more) groups were significantly different. Before each statistical test, data was tested for normality.

Chapter 3: Results

3.1. General architecture of the seedlings

3.1.1 Main stem

It took approximately 2 to 6 weeks for seeds of *T. occidentalis* to germinate. The first structure to sprout out of the soil was a pair of prophylls (cotyledons). The shoot apex was located at the bases of the prophylls where they connected to the hypocotyl. The prophylls were much larger and wider than the leaves that follow. The general shape of the prophylls and the leaves that follow was needle-like. The tip of the prophylls was broader whereas the tip of the leaves was more acute.

Four different phyllotactic patterns (Figure 4A) were observed on the main stem of the seedlings of *T. occidentalis*: tetracussate ((4, 4)), tricussate ((3, 3)), spiral and decussate ((2, 2)). Which spiral pattern specifically (i.e., (m, n) of the pattern) was further determined by histological sections.

The first pattern to emerge was either decussate (the prophylls were considered as the first pair of leaves) (6/93, 6.5%) or tetracussate (the prophylls were considered as two opposite leaves in the first whorl because they were inserted at the same level as the other 2 true leaves) (87/93, 93.5%). If the first pattern to emerge was decussate, the rest of the leaves on the stem would remain as

Figure 4: general architecture of the seedlings of *T. occidentalis*. A: main stem representing various phyllotactic patterns: tetracussate (white portion), tricussate (red portion), spiral (blue portion) and decussate (black portion). P = prophyll. B: side branches representing decussate pattern. S = scale-like leaves; circle: branch exhibiting dimorphic leaf pattern. All scales bars = 0.3 cm.

such. If the first pattern to emerge was tetracussate, after several nodes (normally 1-6, rarely more than 6 (about 5%)), the rest of the leaves on the stem would transition to either decussate (16/87, 18.4%) or tricussate (71/87, 81.6%). If the tetracussate pattern transitioned to decussate, the rest of the leaves on the stem would remain as such. If the tetracussate pattern transitioned to tricussate, the rest of the leaves on the stem would further transition to spiral then to decussate. In this case, the tricussate pattern can be fixed for 1 to as many as 35 nodes. The spiral pattern and the tricussate pattern were difficult to distinguish by simple visual observation, especially when the leaves are packed tightly. They were further determined by histological sections.

The decussate pattern appeared to be the most stable pattern on the main stem of *T. occidentalis*, since all seedlings ultimately reached this pattern. There were 3 pathways to reach the decussate pattern: from the beginning (no pattern transition) (6/93, 6.5%); from tetracussate to decussate (16/93, 17.2%); from tetracussate to tricussate to spiral to decussate (71/93, 76.3%).

The occurrence of the first branching event was recorded for each seedling by determining the number of leaves and number of nodes on the main stem prior to the first branching event. There was no consistent distribution in observed frequencies of leaves produced prior to the first branching event. Seedlings that produced 23 leaves prior to the first branching event were the most common (14/89, 15.7%). Three minor peaks: 20 leaves (10/89, 11.2%), 18 leaves (8/89, 9.0%) and 27 leaves (8/89, 9.0%) were also observed (Figure 5). Seedlings that produced 6 nodes prior to the first branching event were the most common (24/89, 27.0%) (Figure 6).

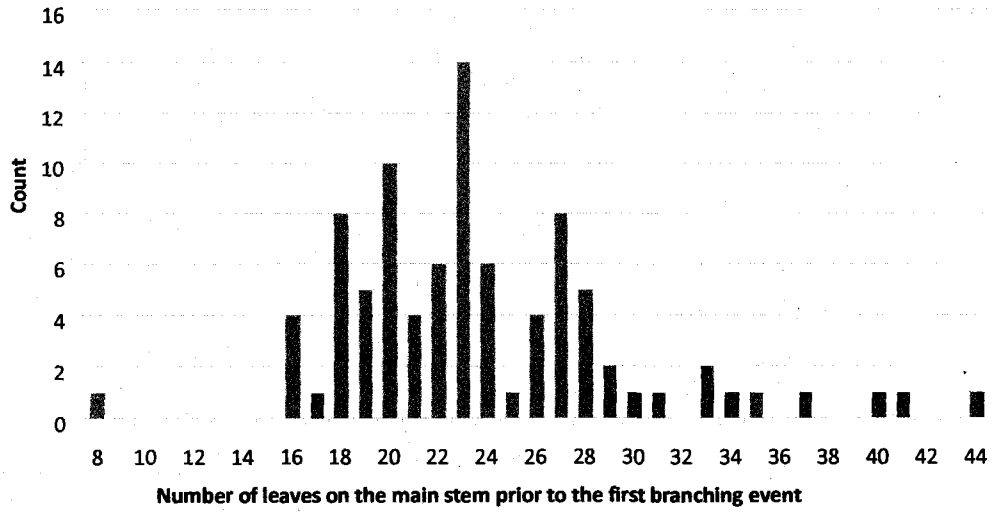

Figure 5: number of leaves on the main stem prior to the first branching event of *T. occidentalis*.

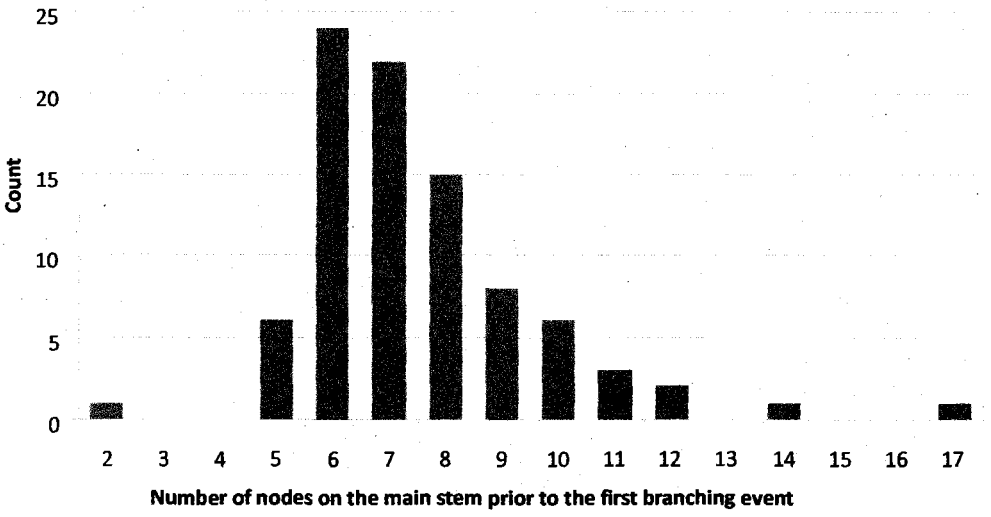

Figure 6: number of nodes on the main stem prior to the first branching event of *T. occidentalis*.

3.1.2 Side branches

Only 1 phyllotactic pattern was observed on the side branches of the seedlings of *T. occidentalis*: decussate ((2, 2)) (Figure 4B). All the second-order branches on the main stem formed a distichous phyllotactic pattern. For each of the second-order branch, 3 pairs of needle-like leaves were formed before the third-order branches grew out and their sizes were about the same as those found on the main stem. After the first third-order branch grew out, another 2 pairs (rarely 4 (about 5%)) of needle-like leaves were formed before a second third-order branch grew out but their sizes were smaller than those of the first 3 pairs. This marked the beginning of the gradual change in leaf shape, which took 4 plastochrones. Between the second third-order branch and the next third-order branch, 2 pairs of leaves were formed; one pair was narrow and cup-shaped (lateral) and the other pair was wide and flat (facial). The narrow and cup-shaped (lateral) pair was adjacent to the second third-order branch and the wide and flat (facial) pair was adjacent to the next third-order branch and this pattern repeated itself.

All the third-order branches on a second-order branch formed a distichous phyllotactic pattern. Between each of the fourth-order branch and the next fourth-order branch, 2 pairs of leaves were formed; one pair was narrow and cup-shaped (lateral) and the other pair was wide and flat (facial). The narrow and cup-shaped (lateral) pair was adjacent to the first fourth-order branch and the wide and flat (facial) pair was adjacent to the next fourth-order branch and this pattern repeated itself. The only exception was that sometimes (about 20%) the first 2 pairs of leaves on the first third-order branch were still needle-like.

The orientation of the first fourth-order branch and most of the other fourth-order branches on each third-order branch was always the same as that of the second-order branch they belonged to. The leaves on the fourth-order branches were characterized by the presence of the same alternating pattern described above. Only a few fifth-order branches were observed and their orientation was the same as that of the third-order branch they belonged to. No sixth-order branches were observed.

3.2 Quantitative description of different phyllotactic patterns

3.2.1 Optical microscopy (OM)

3.2.1.1 Tetracussate pattern of the main stem

The tetracussate pattern only persisted for a very short period of time. Therefore, only 2 or 3 whorls of leaves were available. The first whorl that consisted of a pair of prophylls and the other 2 true leaves was excluded from the analysis because the prophylls were initiated earlier although all of them appeared to be inserted at the same level. In some cases, divergence angle (d) and plastochrone ratio (R) were not measurable because only 1 whorl of leaves was available.

Four shoot apices (4 parastichies on each apex) were examined (Figure 7A). Phyllotactic parameters within each parastichy for the first 2 (or 1) whorls of each apex were listed in Table 1. Divergence angles of leaves in the same whorl were listed in Table 2.

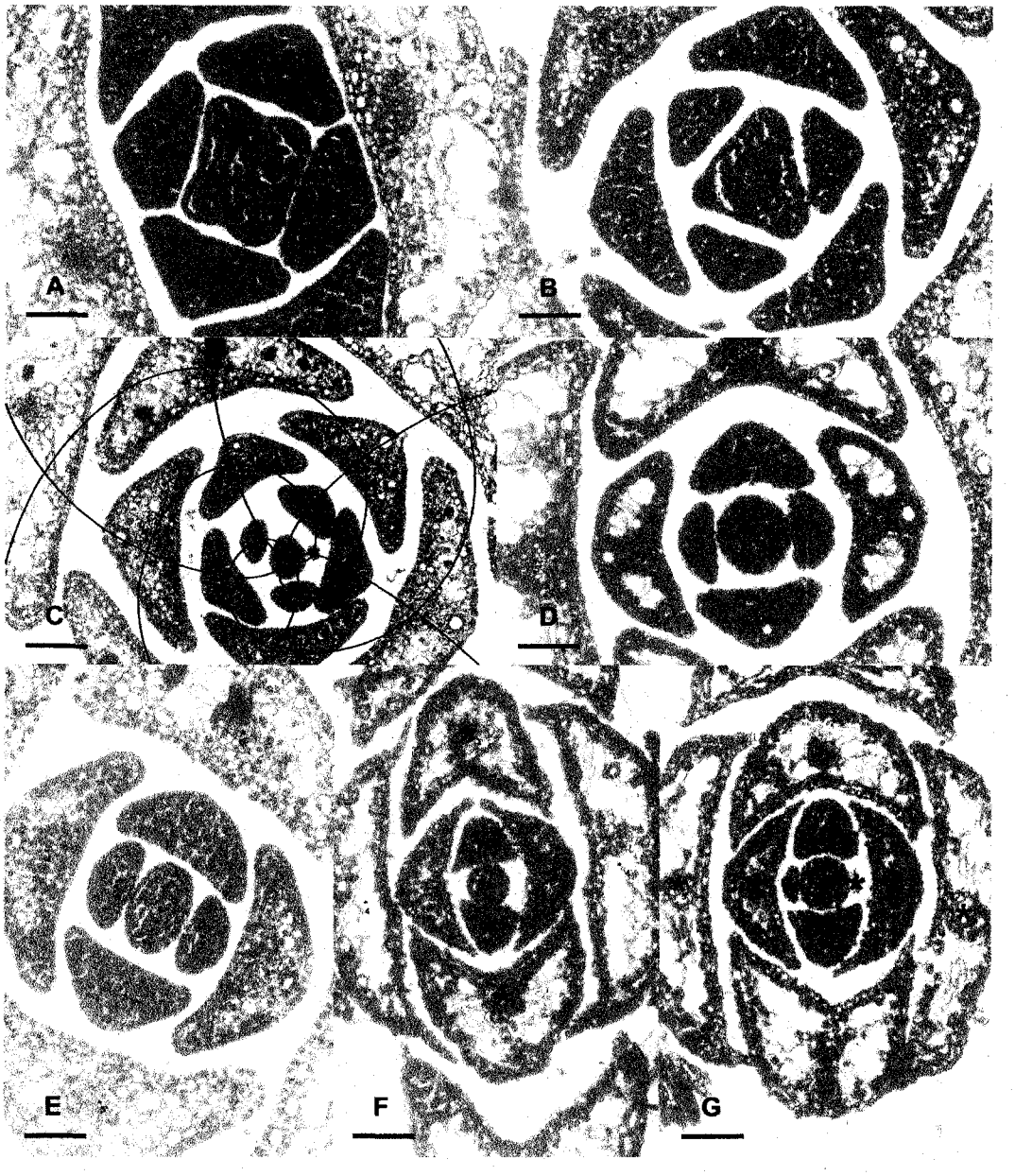

Figure 7: sections of different phyllotactic patterns of *T. occidentalis*. A: tetracussate pattern of the main stem. B: tricussate pattern of the main stem. C: (3, 5) spiral pattern of the main stem; black curve = 3-parastichies; red curve = 5-parastichies. D: decussate pattern of the main stem. E: decussate pattern of the side branches (group of leaf shape unchanged). F: decussate pattern of the side branches (group of first pair of leaves elongated in the radial direction was marked with asterisk sign). G: decussate pattern of the side branches (group of first pair of leaves elongated in the tangential direction was marked with asterisk sign). All scale bars = 82 μm.

Table 1: phyllotactic parameters for the tetracussate pattern of the main stem of *T. occidentalis*.

		d	*R*	*i* (first leaf)	parameter Γ	ψ
Apex 1	Parastichy 1	48.12°	1.17	71.05°	0.89	44.79°
	Parastichy 2	40.19°		80.41°	0.74	48.33°
	Parastichy 3	55.77°		74.18°	1.19	63.11°
	Parastichy 4	27.40°		59.09°	0.96	46.20°
Apex 2	Parastichy 1	NA	NA	70.20°	2.15	83.74°
	Parastichy 2	NA		95.40°	2.58	83.10°
	Parastichy 3	NA		95.54°	2.75	87.94°
	Parastichy 4	NA		92.22°	2.27	98.95°
Apex 3	Parastichy 1	NA	NA	52.68°	1.44	158.04°
	Parastichy 2	NA		76.45°	1.54	101.79°
	Parastichy 3	NA		50.72°	1.04	120.55°
	Parastichy 4	NA		74.92°	1.74	102.70°
Apex 4	Parastichy 1	57.18°	1.15	66.22°	0.95	62.65°
	Parastichy 2	33.42°		69.82°	1.03	59.34°
	Parastichy 3	45.80°		68.79°	1.04	67.20°
	Parastichy 4	39.10°		73.15°	0.96	77.67°

Table 2: Divergence angle of leaves in the same whorl for the tetracussate pattern of the main stem of *T. occidentalis*.

		Between parastichy 1 and 2	Between parastichy 2 and 3	Between parastichy 3 and 4	Between parastichy 4 and 1
Apex 1	Whorl 1	80.63°	86.94°	116.21°	76.22°
	Whorl 2	72.95°	102.97°	88.13°	95.95°
Apex 2	Whorl 1	100.83°	77.17°	113.09°	68.91°
	Whorl 2	NA	NA	NA	NA
Apex 3	Whorl 1	105.03°	77.34°	107.34°	70.29°
	Whorl 2	NA	NA	NA	NA
Apex 4	Whorl 1	117.28°	69.98°	98.01°	74.73°
	Whorl 2	93.92°	81.82°	91.44°	92.82°

The divergence angle (d) for each parastichy varied between 27.40° to 57.18° and the mean divergence angle for all the apices was 43.37°±17.88°. The plastochrone ratio (R) for each apex varied between 1.15 and 1.17 and the mean plastochrone ratio for all the apices was 1.16±0.02. The leaf insertion angle (i) of the first leaf for each parastichy varied between 50.72° and 95.54° and the mean leaf insertion angle of the first leaf for all the apices was 73.18°±13.26°. Parameter Γ for each parastichy varied between 0.74 and 2.75 and the mean value for parameter Γ for all the apices was 1.45±0.65. The apical angle of the SAM (ψ) for each parastichy varied between 44.79° and 158.04° and the mean apical angle of the SAM for all the apices was 75.21°±30.22°. Divergence angle of leaves in the same whorl varied between 68.91° and 117.28°.

3.2.1.2 Tricussate pattern of the main stem

Five shoot apices (3 parastichies on each apex) were examined (Figure 7B). Phyllotactic parameters within each parastichy for the first 4 whorls of each apex were listed in Table 3. Divergence angles of leaves in the same whorl were listed in Table 4.

The mean divergence angle (d) for each parastichy varied between 56.75°±17.59° and 63.88°±21.88° and the mean divergence angle for all the apices was 60.23°±29.33°. The plastochrone ratio (R) for each apex varied between 1.14 and 1.16 and the mean plastochrone ratio for all the apices was 1.15±0.01. The leaf insertion angle (i) of the first leaf for each parastichy varied between 13.89° and 88.13° and the mean leaf insertion angle of the first leaf for all the apices was 59.52°±20.67°. The mean leaf insertion angle of the first 3 leaves for each parastichy

Table 3: phyllotactic parameters for the tricussate pattern of the main stem of *T. occidentalis*.

		d (mean±SD)	*R*	*i* (first leaf)	*i* (mean±SD)	parameter Γ	ψ
Apex 1	Parastichy 1	60.55°±8.30°	1.16	80.32°	101.62°±21.31°	1.89	98.24°
	Parastichy 2	61.14°±3.89°		69.21°	89.93°±18.03°	1.65	82.13°
	Parastichy 3	62.09°±3.44°		58.83°	88.92°±26.11°	1.49	90.44°
Apex 2	Parastichy 1	63.49°±3.40°	1.15	13.89°	68.98°±47.72°	0.32	81.13°
	Parastichy 2	58.22°±7.01°		79.29°	86.44°±7.55°	1.36	94.19°
	Parastichy 3	57.63°±8.50°		35.69°	72.82°±36.33°	1.07	101.63°
Apex 3	Parastichy 1	58.84°±7.32°	1.16	72.29°	79.78°±13.82°	1.25	79.18°
	Parastichy 2	62.31°±7.79°		64.85°	79.68°±13.49°	0.92	74.59°
	Parastichy 3	57.44°±1.63°		67.57°	77.52°±9.91°	1.08	81.48°
Apex 4	Parastichy 1	63.88°±21.88°	1.16	88.13°	87.63°±6.70°	1.70	78.51°
	Parastichy 2	56.75°±17.59°		40.10°	76.45°±31.66°	1.13	88.82°
	Parastichy 3	61.38°±6.23°		66.42°	91.62°±22.55°	1.42	107.05°
Apex 5	Parastichy 1	59.67°±12.64°	1.14	42.12°	75.57°±29.00°	1.15	81.22°
	Parastichy 2	59.91°±13.34°		64.24°	84.85°±17.89°	1.41	81.31°
	Parastichy 3	60.11°±10.45°		49.90°	73.14°±20.34°	1.18	78.16°

Table 4: divergence angle of leaves in the same whorl for the tricussate pattern of the main stem of *T. occidentalis*.

		Between parastichy 1 and 2	Between parastichy 2 and 3	Between parastichy 3 and 1
Apex 1	Whorl 1	121.84°	114.44°	123.72°
	Whorl 2	128.06°	121.52°	110.42°
	Whorl 3	125.58°	114.07°	120.35°
	Whorl 4	123.72°	117.07°	119.21°
Apex 2	Whorl 1	133.71°	124.31°	101.98°
	Whorl 2	125.13°	113.99°	120.88°
	Whorl 3	128.80°	108.46°	122.74°
	Whorl 4	117.89°	122.98°	119.13°
Apex 3	Whorl 1	106.16°	136.63°	117.21°
	Whorl 2	126.49°	123.38°	110.13°
	Whorl 3	122.23°	122.33°	115.44°
	Whorl 4	116.98°	121.90°	121.12°
Apex 4	Whorl 1	109.45°	121.06°	129.49°
	Whorl 2	107.75°	135.65°	116.60°
	Whorl 3	134.93°	113.45°	111.62°
	Whorl 4	88.17°	135.49°	136.34°
Apex 5	Whorl 1	108.63°	114.25°	137.12°
	Whorl 2	105.90°	133.55°	120.55°
	Whorl 3	84.56°	138.48°	136.96°
	Whorl 4	110.32°	114.66°	135.02°

varied between 68.98°±47.72° and 101.62°±21.31° and the mean leaf insertion angle of the first 3 leaves for all the apices was 82.33°±21.96°. Parameter Γ for each parastichy varied between 0.32 and 1.89 and the mean value for parameter Γ for all the apices was 1.27±0.37. The apical angle of the SAM (ψ) for each parastichy varied between 74.59° and 107.05° and the mean apical angle of the SAM for all the apices was 86.54°±9.73°. Divergence angle of leaves in the same whorl varied between 84.56° and 138.48°.

3.2.1.3 Spiral pattern of the main stem

Four shoot apices were examined (Figure 7C). Phyllotactic parameters for the first 6 leaves of each apex were listed in Table 5.

The mean divergence angle (d) for each apex varied between 138.92°±8.04° and 140.41°±10.56° and the mean divergence angle for all the apices was 139.71°±8.61°. Divergence angles of each apex fluctuated around 137.5°, which was typical for most of the spiral patterns. Further analysis of the conspicuous parastichy pair showed this spiral pattern was representative of the (3, 5) pattern (Figure 7C). The plastochrone ratio (R) for each apex varied between 1.12 and 1.20 and the mean plastochrone ratio for all the apices was 1.17±0.03. Values of plastochrone ratios of each apex often fluctuated with a cycle of 1 plastochrone (sometimes 2 (about 15%)). The leaf insertion angle (i) of the first leaf for each apex varied between 37.27° and 69.58° and the mean leaf insertion angle of the first leaf for all the apices was 52.10°±15.98°. The mean leaf insertion angle of the first 3 leaves for each apex varied between 59.26°±27.78° and 82.80°±16.02° and the mean

Table 5: phyllotactic parameters for the (3, 5) spiral pattern of the main stem of *T. occidentalis*.

	d (mean±SD)	*R*	*i* (first leaf)	*i* (mean±SD)	parameter Γ	ψ
Apex 1	140.41°±10.56°	1.12	39.89°	59.26°±27.78°	0.81	117.21°
Apex 2	139.54°±10.93°	1.18	61.67°	76.60°±19.90°	1.79	115.11°
Apex 3	139.98°±7.40°	1.16	37.27°	60.85°±20.69°	0.75	94.75°
Apex 4	138.92°±8.04°	1.20	69.58°	82.80°±16.02°	2.63	80.15°

leaf insertion angle of the first 3 leaves for all the apices was 69.88°±21.16°. Leaf insertion angles of each apex showed a trend where the values increased gradually as expected because each leaf was older than the previous one. Parameter Γ for each apex varied between 0.75 and 2.63 and the value for parameter Γ for all the apices was 1.49±0.89. The apical angle of the SAM (ψ) for each apex varied between 80.15° and 117.21° and the mean apical angle of the SAM for all the apices was 101.81°±17.64°.

3.2.1.4 Decussate pattern of the main stem

Five shoot apices (2 parastichies on each apex) were examined (Figure 7D). Phyllotactic parameters within each parastichy for the first 5 whorls of each apex were listed in Table 6. Divergence angles of leaves in the same whorl were listed in Table 7.

The mean divergence angle (d) for each parastichy varied between 88.94°±6.13° and 91.64°±3.23° and the mean divergence angle for all the apices was 90.48°±4.67°. The plastochrone ratio (R) for each apex varied between 1.19 and 1.21 and the mean plastochrone ratio for all the apices was 1.20±0.01. The leaf insertion angle (i) of the first leaf for each parastichy varied between 48.86° and 103.22° and the mean leaf insertion angle of the first leaf for all the apices was 76.89°±19.37°. The mean leaf insertion angle of the first 3 leaves for each parastichy varied between 87.02°±35.65° and 117.43°±26.77° and the mean leaf insertion angle of the first 3 leaves for all the apices was 99.41°±22.78°. Parameter Γ for each parastichy varied between 0.79 and 1.98 and the mean value for parameter Γ for all the apices was 1.55±0.48. The apical angle of the SAM (ψ)

Table 6: phyllotactic parameters for the decussate pattern of the main stem of *T. occidentalis*.

		d (mean±SD)	*R*	*i* (first leaf)	*i* (mean±SD)	parameter *Γ*	*ψ*
Apex 1	Parastichy 1	91.64°±3.23°	1.21	88.80°	97.50°±7.78°	1.96	69.74°
	Parastichy 2	90.55°±4.05°		87.35°	97.53°±9.31°	1.98	57.61°
Apex 2	Parastichy 1	91.47°±7.37°	1.21	88.74°	117.43°±26.77°	1.96	81.37°
	Parastichy 2	90.83°±2.34°		68.50°	97.05°±25.34°	1.52	59.05°
Apex 3	Parastichy 1	89.49°±5.13°	1.19	78.82°	107.24°±26.57°	1.82	67.96°
	Parastichy 2	91.25°±7.55°		48.86°	89.23°±35.31°	0.79	83.26°
Apex 4	Parastichy 1	89.70°±2.93°	1.19	103.22°	102.31°±15.61°	1.50	45.75°
	Parastichy 2	88.94°±6.13°		50.80°	87.02°±35.65°	0.88	40.01°

Table 7: divergence angle of leaves in the same whorl for the decussate pattern of the main stem of *T. occidentalis*.

		Between parastichy 1 and 2	Between parastichy 2 and 1
Apex 1	Whorl 1	177.83°	182.17°
	Whorl 2	185.38°	174.62°
	Whorl 3	181.63°	178.37°
	Whorl 4	176.96°	183.04°
	Whorl 5	173.37°	186.63°
Apex 2	Whorl 1	177.89°	182.11°
	Whorl 2	177.52°	182.48°
	Whorl 3	166.46°	193.54°
	Whorl 4	163.65°	196.35°
	Whorl 5	175.00°	185.00°
Apex 3	Whorl 1	163.85°	196.15°
	Whorl 2	180.01°	179.99°
	Whorl 3	182.94°	177.06°
	Whorl 4	180.19°	179.81°
	Whorl 5	170.72°	189.28°
Apex 4	Whorl 1	185.72°	174.28°
	Whorl 2	180.44°	179.56°
	Whorl 3	190.45°	169.55°
	Whorl 4	185.02°	174.98°
	Whorl 5	176.17°	183.83°

for each parastichy varied between 40.01° and 83.26° and the mean apical angle of the SAM for all the apices was 63.09°±15.53°. Divergence angle of leaves in the same whorl varied between 163.65° and 196.35°.

3.2.1.5 Decussate pattern of the side branches

Three groups could be further categorized according to the shape of leaves corresponding to the shape of leaves observed on mature plants: (1) leaf shape unchanged (Figure 7E), corresponding to those needle-like l eaves on mature plants; (2) fi rst pair of leaves elongated in the radial direction (Figure 7F), corresponding to those lateral leaves on mature plants; and (3) first pair of leaves elongated in the tangential direction (Figure 7G), corresponding to those facial leaves on mature plants.

Ten shoot apices (2 parastichies on each apex) were examined (apices 1-4: leaf shape unchanged; apices 5-7: first pair of leaves elongated in the radial direction; apices 8-10: first pair of leaves elongated in the tangential direction). Phyllotactic parameters within each parastichy for the first 5 whorls of each apex were listed in Table 8. Divergence angles of leaves in the same whorl were listed in Table 9.

For the group "leaf shape unchanged", the mean divergence angle (*d*) for each parastichy varied between 88.00°±8.24° and 94.10°±8.53° and the mean divergence angle for all the apices was 90.49°±7.29°. The plastochrone ratio (*R*) for each apex varied between 1.17 and 1.23 and the

Table 8: phyllotactic parameters for the decussate pattern of the side branches of *T. occidentalis*.

		d (mean±SD)	*R*	*i* (first leaf)	*i* (mean±SD)	parameter *Γ*	*ψ*
Apex 1	Parastichy 1	91.50°±7.24°	1.18	87.78°	89.96°±25.29°	1.77	63.58°
	Parastichy 2	89.11°±9.54°		49.29°	85.25°±31.64°	1.16	87.69°
Apex 2	Parastichy 1	89.42°±6.62°	1.23	74.59°	88.74°±13.07°	1.11	47.88°
	Parastichy 2	88.00°±8.24°		87.32°	100.84°±14.69°	1.24	43.81°
Apex 3	Parastichy 1	94.10°±8.53°	1.17	81.55°	92.37°±12.55°	1.67	61.91°
	Parastichy 2	91.72°±7.37°		48.26°	80.19°±29.11°	1.02	70.10°
Apex 4	Parastichy 1	90.69°±11.42°	1.18	57.81°	102.08°±38.74°	1.07	42.61°
	Parastichy 2	89.40°±1.49°		76.55°	101.75°±22.26°	1.12	40.01°
Apex 5	Parastichy 1	90.01°±11.80°	1.23	109.38°	113.81°±6.09°	1.36	55.27°
	Parastichy 2	86.44°±9.07°		89.88°	119.19°±26.25°	1.23	69.15°
Apex 6	Parastichy 1	91.31°±3.21°	1.28	121.04°	145.11°±24.45°	2.37	124.43°
	Parastichy 2	88.52°±3.21°		111.89°	126.51°±30.55°	2.43	135.52°
Apex 7	Parastichy 1	89.08°±17.20°	1.21	60.94°	86.82°±23.38°	1.37	89.95°
	Parastichy 2	91.40°±3.28°		86.02°	99.11°±14.27°	1.59	70.58°
Apex 8	Parastichy 1	92.11°±1.58°	1.20	71.11°	110.03°±34.12°	1.45	80.17°
	Parastichy 2	90.31°±2.54°		80.38°	114.12°±29.91°	1.57	75.60°
Apex 9	Parastichy 1	89.37°±6.41°	1.23	67.10°	112.10°±38.98°	1.42	75.15°
	Parastichy 2	90.27°±10.19°		62.87°	107.27°±38.52°	1.39	65.64°
Apex 10	Parastichy 1	93.40°±6.68°	1.21	49.92°	106.25°±52.13°	1.01	36.83°
	Parastichy 2	90.37°±5.26°		67.28°	109.05°±46.62°	1.38	55.69°

Table 9: divergence angle of leaves in the same whorl for the decussate pattern of the side branches of *T. occidentalis*.

		Between parastichy 1 and 2	Between parastichy 2 and 1
	Whorl 1	203.42°	156.58°
	Whorl 2	180.13°	179.87°
Apex 1	Whorl 3	183.32°	176.68°
	Whorl 4	187.12°	172.88°
	Whorl 5	193.77°	166.23°
	Whorl 1	177.16°	182.84°
	Whorl 2	171.61°	188.39°
Apex 2	Whorl 3	176.52°	183.48°
	Whorl 4	182.69°	177.31°
	Whorl 5	171.31°	188.69°
	Whorl 1	181.65°	178.35°
	Whorl 2	177.34°	182.66°
Apex 3	Whorl 3	170.71°	189.29°
	Whorl 4	174.49°	185.51°
	Whorl 5	172.14°	187.86°
	Whorl 1	186.34°	173.66°
	Whorl 2	174.81°	185.19°
Apex 4	Whorl 3	180.07°	179.93°
	Whorl 4	170.35°	189.65°
	Whorl 5	180.38°	179.62°

Table 9 continued

	Whorl 1	189.64°	170.36°
	Whorl 2	161.06°	198.94°
Apex 5	Whorl 3	181.18°	178.82°
	Whorl 4	181.75°	178.25°
	Whorl 5	174.73°	185.27°
	Whorl 1	188.27°	171.73°
	Whorl 2	189.45°	170.55°
Apex 6	Whorl 3	179.72°	180.28°
	Whorl 4	178.57°	181.43°
	Whorl 5	177.07°	182.93°
	Whorl 1	182.07°	177.93°
	Whorl 2	175.00°	185.00°
Apex 7	Whorl 3	182.20°	177.80°
	Whorl 4	170.58°	189.42°
	Whorl 5	190.68°	169.32°
	Whorl 1	180.69°	179.31°
	Whorl 2	180.36°	179.64°
Apex 8	Whorl 3	177.49°	182.51°
	Whorl 4	177.50°	182.50°
	Whorl 5	173.53°	186.47°

Table 9 continued

	Whorl 1	168.28°	191.72°
	Whorl 2	191.86°	168.14°
Apex 9	Whorl 3	181.61°	178.39°
	Whorl 4	176.37°	183.63°
	Whorl 5	171.58°	188.42°
	Whorl 1	178.72°	181.28°
	Whorl 2	184.07°	175.93°
Apex 10	Whorl 3	187.87°	172.13°
	Whorl 4	179.77°	180.23°
	Whorl 5	166.73°	193.27°

mean plastochrone ratio for all the apices was 1.19±0.03. The leaf insertion angle (i) of the first leaf for each parastichy varied between 48.26° and 87.78° and the mean leaf insertion angle of the first leaf for all the apices was 70.39°±16.31°. The mean leaf insertion angle of the first 3 leaves for each parastichy varied between 80.19°±29.11° and 102.08°±38.74° and the mean leaf insertion angle of the first 3 leaves for all the apices was 92.65°±22.33°. Parameter Γ for each parastichy varied between 1.02 and 1.77 and the mean value for parameter Γ for all the apices was 1.27±0.28. The apical angle of the SAM (ψ) for each parastichy varied between 40.01° and 87.69° and the mean apical angle of the SAM for all the apices was 57.20°±16.62°. Divergence angle of leaves in the same whorl varied between 156.58° and 203.42°.

For the group "first pair of leaves elongated in the radial direction", the mean divergence angle (d) for each parastichy varied between 86.44°±9.07° and 91.40°±3.28° and the mean divergence angle for all the apices was 89.46°±8.64°. The plastochrone ratio (R) for each apex varied between 1.21 and 1.28 and the mean plastochrone ratio for all the apices was 1.24±0.04. The leaf insertion angle (i) of the first leaf for each parastichy varied between 60.94° and 121.04° and the mean leaf insertion angle of the first leaf for all the apices was 96.53°±22.01°. The mean leaf insertion angle of the first 3 leaves for each parastichy varied between 86.82°±23.38° and 145.11°±24.45° and the mean leaf insertion angle of the first 3 leaves for all the apices was 115.09°±26.93°. Parameter Γ for each parastichy varied between 1.23 and 2.43 and the mean value for parameter Γ for all the apices was 1.72±0.54. The apical angle of the SAM (ψ) of each parastichy varied between 55.27° and 135.52° and the mean apical angle of the SAM for all the apices was 90.82°±32.47°. Divergence angle of leaves in the same whorl varied between 156.58° and 203.42°.

For the group "first pair of leaves elongated in the tangential direction", the mean divergence angle (d) for each parastichy varied between 89.37°±6.41° and 93.40°±6.68° and the mean divergence angle for all the apices was 90.97°±5.46°. The plastochrone ratio (R) for each apex varied between 1.20 and 1.23 and the mean plastochrone ratio for all the apices was 1.21±0.02. The leaf insertion angle (i) of the first leaf for each parastichy varied between 49.92° and 80.38° and the mean leaf insertion angle of the first leaf for all the apices was 66.44°±10.03°. The mean leaf insertion angle of the first 3 leaves for each parastichy varied between 106.25°±52.13° and 114.12°±29.91° and the mean leaf insertion angle of the first 3 leaves for all the apices was 109.80°±34.33°. Parameter Γ for each parastichy varied between 1.01 and 1.57 and the mean value for parameter Γ for all the apices was 1.37±0.19. The apical angle of the SAM (ψ) for each parastichy varied between 36.83° and 80.17° and the mean apical angle of the SAM for all the apices was 64.85°±16.28°. Divergence angle of leaves in the same whorl varied between 166.73° and 193.27°.

3.2.2 Scanning electron microscopy (SEM)

The values of mean, standard deviation and range for volume of the SAM (v), surface area of the SAM (sa), projected area of the SAM (pa) and height of the SAM (h) for the tetracussate (n = 9) (Figure 8A), tricussate (n = 25) (Figure 8B), spiral (3, 5) (n = 5) (Figure 8C) and decussate (n = 12) (Figure 8D) patterns of the main stem and the decussate pattern of the side branches (n = 47) (Figure 8E) were listed in Table 10. The values of these parameters for each apex for each phyllotactic pattern were listed in Tables 11-15 (Appendix D).

One-way analysis of variance (one-way ANOVA) ($\alpha = 0.05$) showed that for these 4 parameters, these 5 types of phyllotactic patterns were not significantly different (P = 0.875 for *v*; P = 0.962 for *sa*; P = 0.470 for *pa*; P = 0.165 for *h*). Regardless of the phyllotactic patterns involved, two-sample *t*-tests ($\alpha = 0.05$) showed that for these 4 parameters, the apices of the main stem and side branches were not significantly different (P = 0.617 for *v*; P = 0.564 for *sa*; P = 0.198 for *pa*; P = 0.050 for *h*). However, the P-value for *h* was very close to significant (0.050).

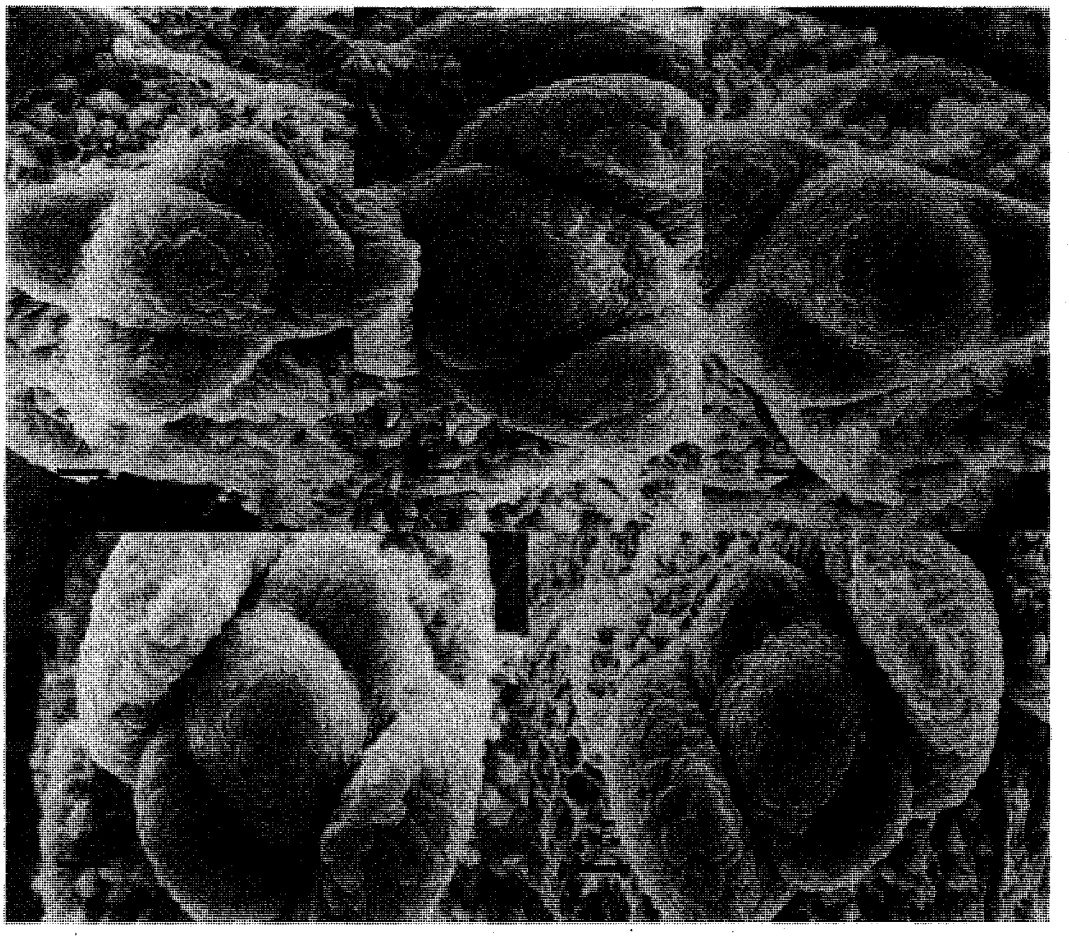

Figure 8: scanning electron micrographs of different phyllotactic patterns of *T. occidentalis*. A: tetracussate pattern of the main stem. B: tricussate pattern of the main stem. C: (3, 5) spiral pattern of the main stem. D: decussate pattern of the main stem. E: decussate pattern of the side branches. All scale bars = 20 μm.

Table 10: the values of mean, standard deviation and range for volume of the SAM (v), surface area of the SAM (sa), projected area of the SAM (pa) and height of the SAM (h) for each phyllotactic pattern of *T. Occidentalis*.

	v (μm^3)		sa (μm^2)		pa (μm^2)		h (μm)	
	mean±SD	range	mean±SD	range	mean±SD	range	mean±SD	range
Tetracussate pattern of the main stem	37280±22558	5024~81721	5194±1618	2497~7991	3248±666	1969~4000	31.40±11.17	18.43~48.37
Tricussate pattern of the main stem	45802±24553	22236~134539	5422±1706	3589~11220	2984±749	2080~5733	34.99±7.56	23.37~53.85
Decussate pattern of the main stem	45696±16794	21819~74711	5474±1504	3499~8361	2789±486	2254~3719	36.88±10.13	19.05~56.32
Spiral (3, 5) pattern of the main stem	41004±14636	19735~56413	5098±1159	3368~6353	2972±452	2310~3481	30.82±7.16	19.39~38.61
Decussate pattern of the side branches	46279±26528	15111~123805	5569±1918	2733~10604	2781±855	1485~5333	38.10±9.48	21.34~61.29

Chapter 4: Discussion

4.1. General architecture of the seedlings

4.1.1 Main stem

The decussate pattern of the side branches of the seedlings of *T. occidentalis* were previously described (Briand *et al.*, 1991; Lacroix *et al.*, 2004). However, phyllotactic patterns of the main stem of the seedlings of *T. occidentalis* and thus the pattern transitions observed in this study have not been documented. The main stem of the seedlings of *T. occidentalis* is characterized by tetracussate, tricussate, spiral and decussate patterns. Therefore, a variety of pattern transitions, such as from tetracussate to tricussate, from tetracussate to decussate, from tricussate to spiral and from spiral to decussate are represented.

It is interesting to note that the pair of prophylls can serve either as a part of the first whorl of a tetracussate pattern or as the first pair of a decussate pattern. This is crucial for determining the pattern that follows. This is probably determined by the relative vertical positioning of the first pair of true leaves in relation to the prophylls. If the first pair of true leaves was inserted at the same level as the prophylls, then a tetracussate pattern will follow, otherwise a decussate pattern will follow. In the case of a decussate pattern, a pseudo-tetracussate pattern will form due to the limited vertical space between leaf pairs at first glance. Whether it is determined intrinsically (e.g., already determined in the seeds) or environmentally (e.g., temperature or the presence or absence

of some growth factors) or both is unknown and needs to be further studied.

One factor that may affect this is the symmetry of the shoot apex. A shoot displays one of the three types of transectional symmetry: radial, bilateral or dorsiventral and can reflect the phyllotactic pattern of the plant (Dengler, 1999). Radial shoots typically have a whorled pattern and usually have symmetrical leaves; bilateral shoots typically have either a distichous or decussate pattern and usually have symmetrical leaves; dorsiventral shoots also typically have either a distichous or decussate pattern but have leaves that differ in size and symmetry (Dengler, 1999). The shoot of *T. occidentalis* shortly after germination has been categorized as bilaterally symmetrical (Nour *et al.*, 1993). However, these authors did not observe the existence of a tetracussate pattern after germination of the seeds. This is probably due to the fact that although the first pair of true leaves is much smaller than the prophylls at initiation (Figure 7A), it will be positioned at the same node as prophylls when the seedling is given some time to grow.

Although there is no consistent distribution in observed frequencies of leaves produced prior to the first branching event, a "peak" at 23 leaves was observed and the frequencies decreased in both directions away from the peak. The same trend in terms of nodes produced prior to the first branching event was also observed. These variations among individual seedlings were observed on seedlings grown under the same condition. It was reported that the formation of buds (and hence side branches) is mainly determined by concentrations of nutrients and metabolites together with auxin as the main regulatory factor and cytokinin as the hormone necessary for cell proliferation (Bessonov *et al.*, 2008). Whether these factors (auxin, cytokinin and others) affect the

numbers of leaves and nodes produced and the branching event needs to be further studied.

4.1.2 Side branches

Trees can be viewed as highly hierarchical systems that can be composed of a finite number of axis orders. Each axis order is characterized by its structure and function. The summation of the architectural characteristics of each axis order results in a description of the architectural unit of the tree (Briand *et al.*, 1991). Although *T. occidentalis* does not fit into any of the 23 architectural models of trees described by Hallé *et al.* (1978), Attims' model is the closest representative (Briand *et al.*, 1991). It has an orthotropic monopodial trunk (main stem), rhythmic growth, diffuse branching, branches are orthotropic (second-order branches) or without a precise direction of growth (third-order to sixth-order branches) and exhibit considerable morphological variation (Briand *et al.*, 1991).

The anisophyllous development on side branches of *T. occidentalis* is obvious. Two types of leaves: narrow and cup-shaped (lateral) leaves and wide and flat (facial) leaves, alternate in a pairwise fashion (Lacroix *et al.*, 2004). Briand *et al.* (1991) studied the entire architectural structures of *T. occidentalis* as well as a variety of morphological features and concluded that the leaves on the main stem and the second-order branches are scale-like whereas the leaves on the third-order to sixth-order branches are dimorphic and alternate in this pairwise fashion. However, it is observed that the leaves on the second-order branches are not always scale-like. The 3 pairs of leaves before the first third-order branch grows out are in fact scale-like and the first 2 (rarely 4

(about 5%)) pairs of leaves after the first third-order branch grows out are scale-like too but their sizes are smaller. This marks the beginning of a gradual change of leaf shape from scale-like leaves to dimorphic leaves, which takes 4 plastochrones. This also indicates that the change in leaf shape is a gradual process at different locations on the branch, not a sudden shift. The details of this gradual change at the level of shoot apical meristem need to be further studied from a morphometric point of view. The dimorphic leaf pattern at the level of the SAM (Figures 7F, 7G) indicates that this is established during early stages of initiation, not later on during leaf development.

It is interesting to note that after the leaves change to the dimorphic leaf pattern, the narrow and cup-shaped (lateral) pair is always adjacent to the older daughter branch and the wide and flat (facial) pair is always adjacent to the younger daughter branch. This probably results from which portion and how much of the SAM will be "assigned" to the production of the daughter branch. This may also be resulting from (or affect) the change of the symmetry in the SAM.

4.2. Quantitative description of different phyllotactic patterns

4.2.1 Empirical relationships

Rutishauser (1998) studied 170 shoot apices of different species of vascular plants and established empirical relationships of different phyllotactic patterns. He concluded that each phyllotactic pattern is characterized by certain ranges of values with respect to plastochrone ratio (R) and leaf

insertion angle (*i*) and divergence angle (*d*) (Rutishauser, 1998). According to the author, the *R* and *i* values of species not yet examined will probably fit in the existing relationship according to their phyllotactic patterns and this hypothesis needs to be further tested (Rutishauser, 1998). For this reason, data obtained from each phyllotactic pattern of *T. occidentalis* will be compared with Rutishauser's empirical relationships.

4.2.1.1 Tetracussate pattern of the main stem

According to Rutishauser (1998), the limits for *d* are 45° (within a parastichy) and 90° (within a whorl); the range for *R* is 1.083 ~ 1.15 and the range for *i* is 52° ~ 90°. For the tetracussate pattern of the main stem of *T. occidentalis*, the ranges for *d* are 27.40° ~ 57.18° (within a parastichy) and 68.91° ~ 117.28° (within a whorl); the range for *R* is 1.15 ~ 1.17 and the range for *i* is 50.72° ~ 95.54°.

For the tetracussate pattern of the main stem of *T. occidentalis*, although the ranges for *d* (both within a parastichy and within a whorl) are very wide, the average value of *d* for all the apices (43.37°) is close to the postulated limit. The range for *R* does not fall in the range outlined by Rutishauser. This may be due to the fact he only examined 1 species and it is plausible that the data for *T. occidentalis* extends this range. Other species may extend this range as well. The range for *i* is a little bit wider than the range outlined by Rutishauser. An *i* value of more than 90° indicates that the leaves of a tetracussate pattern are able to overlap one another to a small extent during later stages of their development.

4.2.1.2 Tricussate pattern of the main stem

According to Rutishauser (1998), the limits for *d* are 60° (within a parastichy) and 120° (within a whorl); the range for *R* is 1.12 ~ 1.49 and the range for *i* is 70° ~ 120°. For the tricussate pattern of the main stem of *T. occidentalis*, the ranges for *d* are 56.75° ~ 63.88° (within a parastichy) and 84.56° ~ 138.48° (within a whorl); the range for *R* is 1.14 ~ 1.16 and the range for *i* is 68.98° ~ 101.62°.

For the tricussate pattern of the main stem of *T. occidentalis*, the range for *d* (within a parastichy) is close to the postulated limit. The range for *d* (within a whorl) is wider than expected. This may be due to the fact the tricussate pattern is undergoing a transition to the spiral pattern and thus forms the pseudo-tricussate pattern. The range for *R* falls in the range outlined by Rutishauser. The lower limit of the range for *i* is a little bit wider than the range outlined by Rutishauser. This may be due to the fact that the methods used are different. Rutishauser (1998) used the maximum *i* value for each species after a certain number of plastochrones. In this study, *i* values were calculated as the average value of the first 3 leaves (except the tetracussate pattern of the main stem). Therefore, it should not be surprising that for the tricussate pattern of the main stem of *T occidentalis*, the lower limit of the range for *i* is wider than the range for *i* outlined by Rutishauser.

4.2.1.3 Spiral pattern of the main stem

According to Rutishauser (1998), the limit for *d* is 137.5° and the range for *d* is 120° ~ 144°; the

range for R is 1.001 ~ 1.67 and the range for i is 4.5° ~ 360°. For the spiral pattern of the main stem of *T. occidentalis*, the range for d is 122.99° ~ 158.58°; the range for R is 1.12 ~ 1.20 and the range for i is 59.26° ~ 82.80°.

For the spiral pattern of the main stem of *T. occidentalis*, the upper limit of the range of d is wider than the range outlined by Rutishauser. This may be due to the fact the range for d outlined by Rutishauser is based on theoretical calculations and it is possible that practical observations do not fall in this range. The ranges for R and i fall in the ranges outlined by Rutishauser.

4.2.1.4 Decussate pattern of the main stem

According to Rutishauser (1998), the limits for d are 90° (within a parastichy) and 180° (within a whorl); the range for R is 1.12 ~ 2.0 and the range for i is 90° ~ 180°. For the decussate pattern of the main stem of *T. occidentalis*, the ranges for d are 88.94° ~ 91.64° (within a parastichy) and 163.65° ~ 196.35° (within a whorl); the range for R is 1.19 ~ 1.21 and the range for i is 87.02° ~ 117.43°.

For the decussate pattern of the main stem of *T. occidentalis*, the range for d (within a parastichy) is very close to the postulated limit. The range for d (within a whorl) is wide. The range for R falls in the range outlined by Rutishauser. The lower limit of the range for i is a little bit wider than the range outlined by Rutishauser. Similarly to what was explained for the tricussate pattern of the main stem, this may be also due to the fact that the methods used are different. Therefore, it should

not be surprising that for the decussate pattern of the main stem of *T. occidentalis*, the lower limit of the range for *i* is wider than the range for *i* outlined by Rutishauser.

4.2.1.5 Decussate pattern of the side branches

According to Rutishauser (1998), the limits for *d* are 90° (within a parastichy) and 180° (within a whorl); the range for *R* is 1.12 ~ 2.0 and the range for *i* is 90° ~ 180°. For the decussate pattern of the side branches of *T. occidentalis*, regardless which group it belongs to according to leaf shape, the ranges for *d* are 86.44° ~ 94.10° (within a parastichy) and 156.58° ~ 203.42° (within a whorl); the range for *R* is 1.17 ~ 1.28 and the range for *i* is 80.19° ~ 145.11°.

For the decussate pattern of the side branches of *T. occidentalis*, regardless of leaf shape, the range for *d* (within a parastichy) is close to its limit. The range for *d* (within a whorl) is wide. The range for *R* falls in the range outlined by Rutishauser. The lower limit of the range for *i* is wider than the range outlined by Rutishauser. Similarly to what was explained for the tricussate and decussate patterns of the main stem, this may be also due to the fact that the methods used are different. Therefore, it should not be surprising that for the decussate pattern of the side branches of *T. occidentalis*, the lower limit of the range for *i* is wider than the range for *i* outlined by Rutishauser.

4.2.2 Theoretical interpretations of the data

4.2.2.1 Divergence angle

The spiral pattern of the main stem of *T. occidentalis* is recognized as a (3, 5) spiral pattern by determining the conspicuous parastichy pair (Figure 7C). It belongs to the Fibonacci sequence (1, 1, 2, 3, 5, 8, ...,) and is characterized by a limit of the divergence angle (*d*) of 137.5°. The observed mean divergence angles for each apex are very close to this limit although a bit higher (140.41°, 139.54°, 139.98°, 138.92°). However, for each apex, there is a fluctuation of *d* around 137.5°. This fluctuation is predicted by the Fundamental Theorem of Phyllotaxis (FTOP), which was developed by Adler (1974, 1977) and later refined by Jean (1988, 1994). The FTOP predicts that for a (3, 5) spiral pattern, its divergence angle will fluctuate between 120° and 144° (Jean, 1994). In *T. occidentalis*, 14 divergence angles out of 20 fall in this range. There are 6 values of divergence angle that are higher than 144° (144.66°, 146.84°, 147.75°, 149.18°, 153.85°, 158.58°) and they are in the range between 120° and 180°, which is predicted by the FTOP for a (2, 3) spiral pattern (Jean, 1994). These higher values of divergence angle are possibly due to the fact that the FTOP is not the only factor that impact divergence angle for a given pattern. A second look of the data shows that the mean value plus the standard deviation of divergence angle for all the apices is higher than 144° (140.41° + 10.56° = 150.97°, 139.54° + 10.93° = 150.47°, 139.98° + 7.40° = 147.38°, 138.92° + 8.04° = 146.96°). If the predictions made by the FTOP are correct, this indicates the contact parastichy pair might be more important than the conspicuous parastichy pair for determining the phyllotactic pattern since (2, 3) is a contact parastichy pair for the spiral

pattern of *T. occidentalis* (Barabé, personal communication).

4.2.2.2 Plastochrone ratio

Just as the divergence angles (*d*) fluctuate around a limit, so do the plastochrone ratios (*R*) with a period of 1 or 2 plastochrones. Theoretical models predict that there is a positive correlation between *d* and *R*, i.e., as *d* increases, *R* decreases, and *vice versa* (Jean, 1994). In *T occidentalis*, 8 of the relationships between *d* and *R* out of 16 match the theoretical prediction. Based on these results, there appears not to be a strong correlation between *d* and *R*. One reason for this lack of correlation may be due to the large value of plastochrone. This was also the case for *Begonia scabrida* (Barabé *et al.*, 2007) and *Euterpe edulis* (Barabé *et al.*, unpublished results). The large value of plastochrone means that the relationship between successive leaves is different, i.e., older leaves are much more developed than the younger leaves.

Theoretically, the plastochrone ratio (*R*) has a value greater than 1. However, in practice, it is possible that the value of *R* can be less than 1, at least in *T. occidentalis*. This was observed not only on the spiral pattern of the main stem, but also on the decussate pattern of the main stem and side branches. These small *R* values are associated with larger *R* values for the previous or next plastochrone (rarely both (about 5%)) and they can be as big as 1.79 (spiral pattern of the main stem), 1.36 (decussate pattern of the main stem) and 1.51 (decussate pattern of the side branches). This indicates that there may be changes in growth rate between successive leaves in *T. occidentalis*, regardless of the phyllotactic pattern involved and whether it is main stem or side

branches. Whether these changes in growth rate can be observed in seedlings need to be studied morphometrically.

For the decussate pattern of the side branches, R values for each apex from the groups "first pair of leaves elongated in the radial direction" and "first pair of leaves elongated in the tangential direction" show a clear fluctuation around the mean R value with a period of 2 plastochrones. The R values for each plastochrone and the mean R values for each apex of both groups are listed in Table 18 (Appendix D). This is because those first narrow and cup-shaped (lateral) leaves grow more in the radial direction than the tangential direction whereas those wide and flat (facial) leaves that follow grow more in the tangential direction than the radial direction. Therefore, the R value between the pair of narrow and cup-shaped (lateral) leaves and the previous pair of wide and flat (facial) leaves is very high and the R value between the pair of wide and flat (facial) leaves and the previous pair of narrow and cup-shaped (lateral) leaves is very low, thereby generating this type of periodicity. The mean R value within a period, however, is in the same range of the R value for the group "leaves shape unchanged".

4.2.2.3 Parameter Γ: **Theoretical development of the results**

The plastochrone ratio (R) can be used for measuring the relative radial distances of primordia as compared to the relative size of the SAM (Rutishauser, 1998) and indirectly estimating the time between the initiation of two successive primordia (Douady and Couder, 1992). Other phyllotactic parameters can be also used for the same purpose, these are: parameter b (van Iterson, 1907) and

parameter Γ (Douady and Couder, 1996b). Parameter b is calculated as:

$$b = d_0/2\pi R_0$$

where d_0 is the diameter of the primordium and the R_0 is the radius of the shoot apex (van Iterson, 1907). Parameter Γ is calculated as:

$$\Gamma = d_0/R_0$$

and

$$\Gamma = \sqrt{(l_1 l_2)}/R_0$$

where l_1 is the tangential length of a primordium and l_2 is the radial length of a primordium (Douady and Couder, 1996b). Γ can be approximated as:

$$\Gamma = l_1/R_0$$

since l_1 is more useful to recognize a leaf primordium at initiation (Snow and Snow, 1933).

Van Iterson (1907) showed that given a value of parameter b and values of divergence angle (d), spiral patterns can be produced accordingly and as the value of parameter b decreases, the number of possible spiral patterns produced increases. By using the similar geometrical control parameter Γ, Douady and Couder (1996b) demonstrated that most of the spiral and whorled phyllotactic patterns can be produced by an iterative process and this process did not produce any unreported pattern.

Theoretically, the range for Γ is 0.8 ~ 0.9 for a tetracussate pattern; 1.05 ~ 1.25 for a tricussate pattern; 1.25 ~ 1.5 for a (3, 5) spiral pattern and 1.5 ~ 1.95 for a decussate pattern (Douady and Couder, 1996b). In *T. occidentalis*, the range of Γ for the tetracussate pattern is 0.74 ~ 2.75 and the

mean value is 1.45; the range of Γ for the tricussate pattern is 0.32 ~ 1.89 and the mean value is 1.27; the range of Γ for the (3, 5) spiral pattern is 0.75 ~ 2.63 and the mean value is 1.49; the range of Γ for the decussate pattern (regardless whether it is main stem or side branches) is 0.79 ~ 2.43 and the mean value is 1.47.

The theoretical prediction and the mean value of Γ for the tetracussate pattern do not match. The theoretical predictions and the mean values of Γ for the tricussate pattern and the decussate pattern do not match but are very close. This poor correlation is probably due to the fact that the limited number of apices studied. However, the theoretical prediction and the mean value of Γ for the (3, 5) spiral pattern of *T. occidentalis* match. This was also the case for *Anagallis arvensis* (Kwiatwoska and Dumais, 2003; calculated by Barabé *et al.*, 2007), *Begonia scabrida* (Barabé *et al.*, 2007) and *Euterpe edulis* (Barabé *et al.*, unpublished results). However, in the former 2 situations, the value of parameter Γ should be multiplied by 2 because it was calculated as:

$$\Gamma = l_1/d_0$$

where d_0 is the diameter of the SAM. This does not change the results and interpretations because the values of parameter Γ will still be within the spiral range and the distichous range, respectively (Barabé *et al.*, 2007). The ranges for parameter Γ observed in *T. occidentalis* are much wider than those of the theoretical predictions. This is probably due to the fact that while the size of the SAM is relatively stable, the size of the youngest primordium will vary considerably depending on the stage of initiation used. Whether this statement is true needs to be further examined in other species.

Parameter Γ can be also calculated as:

$$\Gamma = 2\sin(i_1/2)$$

where i_1 is the leaf insertion angle of the first primordium (Douady and Couder, 1996b). Therefore, 3 different equations can be used to calculate parameter Γ:

$$\Gamma = l_1/R_0 \text{ (commonly used)}$$

$$\Gamma = \sqrt{(l_1 l_2)}/R_0 \text{ (theoretical)}$$

$$\Gamma = 2\sin(i_1/2) \text{ (theoretical)}$$

All these parameters: l_1, l_2, R_0 and i_1 can be measured easily. The values of parameter Γ calculated by these 3 equations for 63 primordia (regardless of the phyllotactic pattern involved) are listed in Table 16 (Appendix D). A two-sample paired *t*-test ($\alpha = 0.05$) showed that the values of l_1/R_0 and $2\sin(i_1/2)$ are significantly different ($P = 0.000$) and the value of l_1/R_0 is greater than the value of $2\sin(i_1/2)$. Another two-sample paired *t*-test ($\alpha = 0.05$) showed that the values of $\sqrt{(l_1 l_2)}/R_0$ and $2\sin(i_1/2)$ are not significantly different ($P = 0.808$). These results show that using $\sqrt{(l_1 l_2)}/R_0$ is a better match to $2\sin(i_1/2)$ than l_1/R_0. This may be due to the fact that the substitution of $\sqrt{(l_1 l_2)}$ by l_1 is not valid and indicates that using $\sqrt{(l_1 l_2)}/R_0$ instead of l_1/R_0 is a more accurate way to calculate parameter Γ, at least for *T. occidentalis*. Whether the assumption that $\sqrt{(l_1 l_2)}$ can be substituted by l_1 to calculate parameter Γ is valid or not needs to be further studied both theoretically and empirically.

4.2.2.4 Pseudowhorls

The phenomenon of pseudowhorl was described (Bravais and Bravais, 1837) and studied by

various authors (Schoute, 1925, 1936; England and Tolbert, 1964; Kwiatkowska, 1995, 1999; Lyndon, 1978) and the mechanism of their formation has not been fully investigated yet. Pseudowhorls are composed of leaves attached at almost same levels and separated by single fully elongated internodes (Kwiatkowska, 1999). The number of leaves per pseudowhorl, regardless of the phyllotactic pattern involved, is the number of leaves in physical contact with the SAM (Kwiatkowska, 1999). In spiral patterns, a pseudowhorl is composed of successive leaves on the genetic spiral and the number of leaves per pseudowhorl equals the highest of the numbers of contact parastichies. In whorled patterns, a pseudowhorl is composed of leaves on 2 adjacent whorls initiated at almost the same time and the number of leaves per pseudowhorl equals the number of orthostichies (Kwiatkowska, 1999).

It was reported that in *Peperomia verticillata*, a decussate pattern can form pseudo-tetracussate patterns; a tricussate pattern can form pseudo-hexacussate patterns and a Fibonacci pattern can form pseudo-decussate, pseudo-tricussate and pseudo-pentacussate patterns. Regardless of the phyllotactic pattern involved, the plastochrone ratio (R) values for the pseudowhorls are greater than the R values of the true whorls (Kwiatkowska, 1999).

The tetracussate pattern of the main stem of *T. occidentalis* does not form pseudowhorls because each true whorl of leaves almost encircles the SAM and the next true whorl of leaves is not in physical contact with the shoot apex (figure 7A). It is also important to note that the tetracussate pattern observed is not a pseudo-tetracussate pattern formed by a decussate pattern because there are 8 orthostichies observed (figure 7A) instead of 4.

The tricussate pattern of the main stem of *T. occidentalis* forms pseudo-hexacussate pattern. The *R* value of the true whorls and the *R* value of the corresponding pseudowhorls for each apex are listed in Table 17 (Appendix D). A two-sample *t*-test ($\alpha = 0.05$) showed that The *R* value of the true whorls and the *R* value of the corresponding pseudowhorls for the tricussate pattern of the main stem of *T. occidentalis* are not significantly different (P = 0.056). This is not in accordance with the results suggested by Kwiatkowska (1999) where there were significant difference between true whorls and the corresponding pseudowhorls for the tricussate pattern.

The decussate pattern (regardless whether it is main stem or side branches) of *T. occidentalis* forms pseudo-tetracussate pattern. The *R* value of the true whorls and the *R* value of the corresponding pseudowhorls for each apex are listed in Table 17 (Appendix D). A two-sample *t*-test ($\alpha = 0.05$) showed that the *R* value of the true whorls and the *R* value of the corresponding pseudowhorls for the decussate pattern (regardless whether it is main stem or side branches) of *T. occidentalis* are significantly different (P = 0.000) and the *R* value of the corresponding pseudowhorls are greater than the *R* value of the true whorls. This is in accordance with the results suggested by Kwiatkowska (1999) where there were significant difference between true whorls and the corresponding pseudowhorls for the decussate pattern..

The (3, 5) spiral pattern of the main stem of *T. occidentalis* forms pseudo-pentacussate pattern. However, due to the limited number of primordia studied, it is impossible to calculate *R* values for the pseudowhorls. It is also possible that the (3, 5) spiral pattern of the main stem of *T. occidentalis* forms pseudo-tricussate pattern because some of the divergence angles measured

(Table 7: apex 4, whorl 4; apex 5; whorl 3) are very similar to the theoretical calculations of pseudo-tricussate pattern formed by spiral patterns (Kwiatkowska, 1999).

4.2.3 Pattern transitions

4.2.3.1 Discontinuous transitions

There are generally two types of phyllotactic pattern transitions: continuous and discontinuous (Zagórska-Marek, 1987). A continuous transition is a transition within the same type of patterns but only the order changes, i.e., (m, n) of the pattern changes along the same sequence and its quality does not change (e.g., from a (2, 3) spiral pattern to a (3, 5) spiral pattern). A discontinuous transition is a transition between different types of patterns, i.e., (m, n) of the pattern changes between different sequences (e.g., from a Fibonacci pattern to a decussate pattern or a Lucas pattern).

Phyllotactic pattern transitions have been mainly studied by recording changes in contact parastichy pairs and this initiated the studies of phyllotactic pattern transitions between various spiral patterns (Zagórska-Marek, personal communication). Discontinuous transitions have been studied in *Abies balsamea* (Zagórska-Marek, 1985, 1987), *Epilobium hirsutum* (Meicenheimer, 1981, 1982, 1998), *Linum usitatissimum* (Meicenheimer, 1981, 1998) and *Magnolia* (Zagórska-Marek, 1987, 1994; Zagórska-Marek and Wiss, 2003). The discontinuous transition from decussate to spiral was studied the most in comparison to other types of discontinuous

transitions. However, there is no complete analysis of a discontinuous transition from spiral to decussate.

All phyllotactic pattern transitions on the main stem of *T. occidentalis*: from tetracussate to tricussate (from (4, 4) to (3, 3)); from tetracussate to decussate (from (4, 4) to (2, 2)); from tricussate to spiral (from (3, 3) to (3, 5)) and from spiral to decussate (from (3, 5) to (2, 2)), are discontinuous phyllotactic pattern transitions. The most common discontinuous phyllotactic pattern transition (especially in eudicotyledons) is from decussate to spiral (Meicenheimer, 1998). The phyllotactic pattern transitions observed on the main stem of *T. occidentalis* are relatively rare and constitute an important framework for future studies and theoretical validation of models.

For the decussate to spiral transition, there are two genetic spirals (parastichies) before the transition and only one genetic spiral after the transition. This genetic spiral is the continuation of one of the genetic spirals of the decussate pattern (Meicenheimer, 1998). The genetic spirals of the decussate pattern before the transition are arbitrarily determined by whether or not they persist in the genetic spiral of the spiral pattern after the transition. Before the transition, the primordia in the genetic spiral of the decussate pattern that goes into the genetic spiral of the spiral pattern are designated by T - 1, T - 2 and so on and the primordia in the genetic spiral of the decussate pattern that is terminated as a result of the transition are designated by T - 1', T - 2' and so on. After the transition, the primordia are designated by T, T + 1, T + 2, and so on. The T + 1 primordium can be considered as the primordium that would have continued the genetic spiral of the decussate pattern if the transition had not occurred (Meicenheimer, 1998).

In *L. usitatissimum*, before the transition, a comparison of the divergence angles indicates that primordia along the two genetic spirals were positioned symmetrically. After the transition, there appears to be a temporary delay between the initiation of the first two primordia in the spiral pattern (T and $T + 1$) which would have been simultaneously initiated if the transition had not occurred. The divergence angle between the last primordium in the decussate pattern (T - 1) and the first primordium in the spiral pattern (T) increased significantly. The divergence angle between the prime primordium in the decussate pattern (T - 1') and the second primordium in the spiral pattern (T + 1), which can be considered as a primordium of the decussate pattern if the transition had not occurred, decreased significantly. It is also noted that the divergence angle fluctuates for several plastochrones after the transition. Before the transition, a comparison of the plastochrone ratios indicates that primordia along the two genetic spirals are expanding at the same relative radial rates. After the transition, a comparison of the plastochrone ratios indicates that the first primordium in the spiral pattern (T) is initiated at a larger radial distance from the center of the SAM than would be expected if the transition had not occurred whereas the second primordium in the spiral pattern (T + 1) is initiated at an expected radial distance if the transition had not occurred. A comparison of the values of parameter Γ (calculated as: $\Gamma = \sqrt{(l_1 l_2)}/R_0$) before and after the transition shows a significant difference, which indicates a shape change of the primordium. A comparison of the half apical angle of the SAM ($\psi/2$) before and after the transition shows no significant difference. These results indicate that the first two primordia in the spiral pattern (T and T + 1) break the symmetry of the SAM and a sector of meristem is effectively lost from one region to another, which will initiate the third primordium in the spiral pattern (T + 2) (Meicenheimer, 1998).

In *E. hirsutum*, before the transition, a comparison of the divergence angles indicates that primordia along the two genetic spirals were positioned symmetrically. After the transition, the divergence angle between the last primordium in the decussate pattern (T - 1) and the first primordium in the spiral pattern (T) increased significantly. The divergence angle between the last primordium in the decussate pattern (T - 1') and the second primordium in the spiral pattern (T + 1) decreased significantly. A comparison of the plastochrone ratios before and after the transition shows a slight increase between the last primordium in the decussate pattern (T - 1) and the first primordium in the spiral pattern (T) and between the first primordium in the spiral pattern (T) and the second primordium in the spiral pattern (T + 1). These increases are probably related to the fact that during the transition the volume of the shoot apical meristem (SAM) increased. The volume increase of the SAM to some extent diminishes the relative radial spacing between the last primordium in the decussate pattern (T - 1) and the first primordium in the spiral pattern (T). This indicates that the size of the SAM increases proportionally with the plastochrone ratio but the shape of the SAM does not change much during the transition. A comparison of the values of parameter Γ (calculated as: $\Gamma = \sqrt{(l_1 l_2)}/R_0$) before and after the transition shows no significant difference. The comparison of the half apical an gle of the SAM ($\psi/2$) before and after the transition shows it increased after transition. These also point to the expansion of the SAM during the transition but the shape of the SAM before and after the transition is similar (Meicenheimer, 1998).

In *T. occidentalis*, unfortunately, not a single transition in pattern was captured on one slide. Therefore, it is impossible to determine which genetic spiral(s) before the transition is (are)

terminated as the result of the transition and which genetic spiral(s) before the transition persist(s). However, it is possible to compare different phyllotactic patterns using apical angle of the SAM (ψ) (Tables 1-5), which can to some extent reflect the change in the shape of the SAM in general.

4.2.3.2 Apical angle of the SAM

One-way analysis of variance (one-way ANOVA) ($\alpha = 0.05$) showed that for apical angle of the SAM (ψ), these 5 types of phyllotactic patterns are significantly different ($P = 0.018$). Further Tukey's multiple comparison ($\alpha = 0.05$) showed that the tricussate pattern of the main stem and the decussate pattern of the main stem are significantly different ($P = 0.003$) and the tricussate pattern of the main stem is greater; the tricussate pattern of the main stem and the decussate pattern of the side branches are significantly different ($P = 0.012$) and the tricussate pattern of the main stem is greater; the (3, 5) spiral pattern of the main stem and the decussate pattern of the main stem are significantly different ($P = 0.014$) and the (3, 5) spiral pattern of the main stem is greater; the (3, 5) spiral pattern of the main stem and the decussate pattern of the side branches are significantly different ($P = 0.028$) and the (3, 5) spiral pattern of the main stem is greater. These results will be further compared with those from scanning electron microscopy.

4.2.4 Considering the actual three-dimensional shape of the shoot apex

4.2.4.1 A connection between the new parameters and the classical ones

The growth of the shoot apical meristem (SAM) is a three-dimensional event and the phenomenon of phyllotaxis should therefore be a three-dimensional study of the SAM. For a very long time, the phenomenon of phyllotaxis was studied and interpreted two-dimensionally followed by the influence of the "centric representation" (Church, 1904; Richards, 1948). This was due in great part to the limitation of techniques. Three-dimensional studies of phyllotaxis are few compared to two-dimensional studies of phyllotaxis. The only parameter used to date to characterize the actual three-dimensional shape of the shoot apex is the apical angle of the SAM (ψ). It was studied theoretically (van Iterson, 1907; Richards, 1951; Douady and Couder, 1996b) and experimentally (Meicenheimer, 1998). However, it is difficult to connect it with other phyllotactic parameters theoretically.

The scanning electron microscopy three-dimensional (SEM 3D) reconstruction method and 4 additional parameters: volume of the SAM (v), surface area of the SAM (sa), projected area of the SAM (pa) and height of the SAM (h) were introduced for the first time to the study of phyllotaxis. These parameters can help to describe the actual three-dimensional shape of the SAM.

To link these 4 parameters and other parameters (apical angle of the SAM (ψ), radius of the SAM (R_0) and plastochrone ratio (R)) together, it is necessary to make the assumption that the SAM can

be approximated as a cone (more accurately a right circular cone) (Figure 9). This assumption was already used by van Iterson (1907), Richards (1951) and Douady and Couder (1996b). Therefore, ψ is the apical angle of the cone; R_0 is the radius of the basal area of the SAM and the cone; v is the volume of the SAM; sa is the lateral area of the SAM; pa is the basal area of the SAM and the cone and h is the height of the SAM. If we take the assumption under consideration, the following equations can be established:

$$\tan(\psi/2) = R_0/h$$

$$pa = \pi R_0^2$$

$$v = \pi R_0^2 h/3$$

$$sa = \pi R_0 \sqrt{(R_0^2 + h^2)}$$

$$h = 3v/pa$$

Although R_0 can be measured using histological sections, it is better to calculate as:

$$R_0 = \sqrt{(pa/\pi)}$$

because R_0 obtained by measurement is always smaller than R_0 in reality due to the fact that the section plane is usually above the basal plane of the SAM. Consequently, v, sa and h of the cone can be also calculated using calculated value of R_0 and above equations.

Regardless of the phyllotactic pattern involved, measured values of v, sa and h of the SAM and calculated values of v, sa and h of the cone for each apex are listed in Table 19 (Appendix D). Two-sample paired t-tests ($\alpha = 0.05$) showed that measured values of v, sa and h of the SAM and calculated values of v, sa and h of the cone are significantly different ($P = 0.000$ for all of them) and measured values of v and sa of the SAM are greater than calculated values of v and sa of the

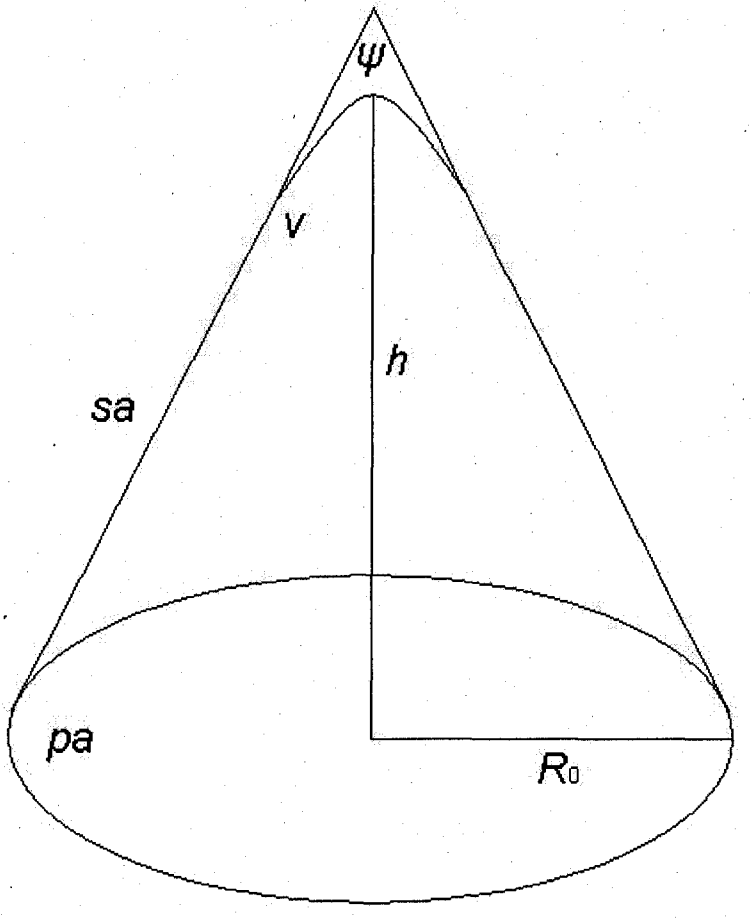

Figure 9: the assumption that approximates the SAM as a cone. The SAM and the cone share the basal area. Ψ: apical angle of the cone; R_0: radius of the basal area of the SAM and the cone; *v*: volume of the SAM; *sa*: lateral area of the SAM; *pa*: basal area of the SAM and the cone; *h*: height of the SAM.

cone whereas calculated value of *h* of the cone is greater than measured value of *h* of the SAM.

These differences show that the assumption that the SAM can be approximated as a cone may not be completely valid. Therefore, further adjustments such as approximating the SAM as a paraboloid may need to be made. This suggestion was also made by Douady and Couder (1996b).

4.2.4.2 Apical angle of the SAM

One-way analysis of variance (one-way ANOVA) ($\alpha = 0.05$) showed that for calculated apical angle of the SAM (ψ) (Table 19) (Appendix D), these 5 types of phyllotactic patterns are also significantly different ($P = 0.000$). Further Tukey's multiple comparison ($\alpha = 0.05$) showed that the tetracussate pattern of the main stem and the tricussate pattern of the main stem are significantly different ($P = 0.031$) and the tetracussate pattern of the main stem is greater; the tetracussate pattern of the main stem and the decussate pattern of the main stem are significantly different ($P = 0.011$) and the tetracussate pattern of the main stem is greater; the tetracussate pattern of the main stem and the decussate pattern of the side branches are significantly different ($P = 0.012$) and the tetracussate pattern of the main stem is greater; the tricussate pattern of the main stem and the decussate pattern of the side branches are significantly different ($P = 0.024$) and the tricussate pattern of the main stem is greater. These results combined with those from optical microscopy show that as the seedlings grow and undergo pattern transitions, apical angle of the SAM (ψ) decreased significantly in both main stem and side branches of *T. occidentalis*.

4.2.4.3 Using new parameters to compare phyllotactic patterns

Although One-way analyses of variance (ANOVA) indicate there is no significant difference between different phyllotactic patterns for volume of the SAM (*v*), surface area of the SAM (*sa*), projected area of the SAM (*pa*) and height of the SAM (*h*), it is noted that the ranges for these parameters are very wide. This is probably due to the fact that the SAM varies depending on the stage of initiation of the youngest primordia at periphery of the SAM. Identifying specific stages of initiation, which was used by Lacroix *et al* (2004), might help to circumscribe the ranges of measured values a bit more.

The fact that the apices with different phyllotactic patterns do not differ in these 4 parameters indicates that what may change during a phyllotactic pattern transition is the size of the primordia, which might be affected by the auxin sink around the primordia (Zagórska-Marek, personal communication). Therefore, if these 4 new parameters would have been also measured for each primordium, it would have been possible to determine if the size of the primordia changes quantitatively between different phyllotactic patterns.

According to Richards (1948, 1951), each plastochrone ratio (*R*) represents the ratio of two areas: area of the SAM and area of the primordium at initiation. Richard's area ratio (*A*) is defined as the ratio of the mean area of the SAM to the mean area of the primordium at initiation and it is calculated as:

$$A = 1/(2\ln R)$$

The minimum area ratio (*MiA*) is defined as the ratio of the minimum area of the SAM just after the initiation of a new primordium to the area of the primordium at initiation and it is calculated as:

$$MiA = 1/(R^2 - 1)$$

The maximum area ratio (*MaA*) is defined as the ratio of the maximum area of the SAM just before the initiation of a new primordium to the area of the primordium at initiation and it is calculated as:

$$MaA = R^2/(R^2 - 1)$$

Therefore, if these 4 new parameters would have been also measured for each primordium at initiation, it would have been possible to calculate *R* by using the above equations and further evaluate the relationships between *R*, *A*, *MiA* and *MaA*. In addition to using the cone assumption, this is a second way to connect the new parameters and the classical ones, especially *R*.

The SEM 3D reconstruction method is new and very promising. It can facilitate the study of phyllotaxis from a three-dimensional perspective and is of importance to establish new models of phyllotaxis and test old ones in a variety of species. The advantage of this method is that the parameters related to any portion of the SAM (or primordia) can be easily measured. However, for species with large SAM, it is not very convenient because only the SAM can be measured by the software accurately; the periphery is treated as an outlier by the algorithm of the software. Consequently, it takes time to measure the parameters of the primordia for species with large SAM because the series of micrographs for each primordium would need to be taken separately. Therefore, it is recommended that in future studies this method could be used initially in species

with small SAM.

Chapter 5: Conclusions

5.1 General architecture of the seedlings

Four phyllotactic patterns were observed on the main stem of *T. occidentalis*: tetracussate, tricussate, (3, 5) spiral and decussate. The first pattern to emerge was either decussate or tetracussate. If the first pattern to emerge was decussate, the rest of the leaves on the stem would remain as such. If the first pattern to emerge was tetracussate, the rest of the leaves on the stem would transition to either decussate or tricussate. If the tetracussate pattern transitioned to decussate, the rest of the leaves on the stem would remain as such. If the tetracussate pattern transitioned to tricussate, it would further transition to (3, 5) spiral then to decussate. The decussate pattern appears to be the most stable pattern. Only 1 phyllotactic pattern was observed on the side branches of *T. occidentalis*: decussate.

5.2 Optical microscopy (OM)

5.2.1 Empirical relationships

The range for R for the tetracussate pattern of the main stem of *T. occidentalis* does not fall in the range outlined by Rutishauser (1998) points to the fact that the range might need to be extended to more present species. The range for d for the spiral pattern of the main stem of *T. occidentalis* is wider than the range outlined by Rutishauser (1998). Theoretical prediction (Jean, 1994) indicates

that a spiral pattern has a broader range for d (120° to 180°) and this range should be more appropriate for the empirical relationship. The lower limits of the range for i for the tricussate and decussate patterns of the main stem and the decussate pattern of the side branches of *T. occidentalis* are wider than the ranges outlined by Rutishauser (1998). This may be due to the fact the methods used are different. Rutishauser (1998) used the maximum i value for each species after a certain number of plastochrones. In this study, i values were calculated as the average value of the first 3 leaves (except the tetracussate pattern of the main stem). Therefore, it should not be surprising that for various patterns, the lower limit of the range for i is wider than the range for i outlined by Rutishauser.

5.2.2 Theoretical interpretations of the data

The spiral pattern of the main stem of *T. occidentalis* is recognized as a (3, 5) spiral pattern by determining the conspicuous parastichy pair. Its divergence angles and plastochrone ratios fluctuate around limits. The Fundamental Theorem of Phyllotaxis predicts that for a (3, 5) spiral pattern, the fluctuation of the divergence angles is between 120° and 144° (Jean, 1994). However, in *T. occidentalis*, some of the divergence angles did not fall in this range. This is probably due to the fact that the FTOP is not the only factor that impacts divergence angle for a given pattern. This indicates that the contact parastichy pair might be more important than the conspicuous parastichy pair for determining the spiral phyllotactic pattern (Barabé, personal communication).

The comparison of 3 ways to calculate parameter Γ indicates that using $\Gamma = \sqrt{(l_1 l_2)}/R_0$ is a better

way to calculate it in *T. occidentalis*. This may be due to the fact that the substitution of $\sqrt{(l_1 l_2)}$ by l_1 is not valid. Whether the assumption that $\sqrt{(l_1 l_2)}$ can be substituted by l_1 to calculate parameter Γ is valid or not needs to be further studied both theoretically and empirically.

5.2.3 Pattern transitions

Four phyllotactic pattern transitions were observed: from tetracussate to decussate, from tetracussate to tricussate, from tricussate to (3, 5) spiral and from (3, 5) spiral to decussate. These pattern transitions are all discontinuous transitions and are relatively rare and important for future studies and helping to validate models that can predict or produce particular pattern transitions. Mathematical calculations and statistical tests indicate that as the seedlings grow and undergo pattern transitions, the apical angle of the SAM (ψ) decreased significantly in both main stem and side branches of *T. occidentalis*.

5.3 Scanning electron microscopy (SEM)

The scanning electron microscopy three-dimensional (SEM 3D) reconstruction method and 4 additional parameters: volume of the SAM (v), surface area of the SAM (sa), projected area of the SAM (pa) and height of the SAM (h) were introduced for the first time to the study of phyllotaxis. These 4 parameters can help to describe the actual three-dimensional shape of the SAM. Mathematical calculations and statistical tests indicate that the assumption that the SAM can be approximated as a cone may not be completely valid and further adjustments such as

approximating the SAM as a paraboloid may need to be made. The analyses of these 4 parameters indicate they are not significantly different for different phyllotactic patterns of *T occidentalis*. This indicates that what may change during a phyllotactic pattern transition is the size of the primordia.

5.4 General conclusion

In this study, the general architecture of seedlings of *T. occidentalis* and leaf shape changes that take place in various axis orders were described; the mathematical basis of each phyllotactic pattern in seedlings of *T. occidentalis* as well as the pattern transitions were documented using histological methods.

In this study, the SEM 3D reconstruction method is used to study phyllotaxis for the first time and it can help to advance the study of phyllotaxis from the two-dimensional perspective to the three-dimensional perspective, which is one step closer to the actual shape of the SAM. The newly introduced parameters can be linked to the existing parameters theoretically. Therefore, it is useful to examine existing hypotheses and models. In this study, only the SAM is analyzed. In future studies, however, both the SAM and the primordia should be analyzed using this method in order to make comparisons between them since it is suggested that the relative size difference between them is the most important factor to control the state of a pattern.

References

Adler, I., 1974. *A Model of Contact Pressure in Phyllotaxis*. Journal of Theoretical Biology. 45: 1-79.

Adler, I., 1977. *The Consequences of Contact Pressure in Phyllotaxis*. Journal of Theoretical Biology. 65: 29-77.

Adler, I., Barabé, D. and Jean, R., 1997. *A History of the Study of Phyllotaxis*. Annals of Botany. 80: 231-244.

Atela, P., Golé, C. and Hotton, S., 2002. *A Dynamical System for Plant Pattern Formation: a Rigorous Analysis*. Journal of Nonlinear Science. 12: 641-676.

Barabé, D., 1991. *Chaos in Plant Morphology*. Acta Biotheoretica. 39: 157-159.

Barabé, D., 2006. *Stochastic Approaches in Phyllotaxis*. Canadian Journal of Botany. 84: 1675-1685.

Barabé, D. and Jeune, B., 2004. *The Use of Entropy to Analyze Phyllotactic Mutants: a Theoretical Analysis*. Plant Cell. 16: 804-806.

Barabé, D., Lacroix, C. and Jeune, B., 2007. *Following the Initiation and Development of Individual Leaf Primordia at the Level of the Shoot Apical Meristem: the Case of Distichous in* Begonia. Annals of Botany. 99: 555-560.

Beck, C., 2005. *An Introduction to Plant Structure and Development: Plant Anatomy for the Twenty-first Century*. Cambridge University Press: New York.

Bell, A., 1991. *Plant Form: an illustrated Guide to Flowering Plant Morphology*. Oxford University Press: New York.

Berleth, T., Scarpella, E. and Prusinkiewicz, P., 2007. *Toward the Systems Biology of Auxin-transport-mediated Patterning*. Trends in Plant Science. 12: 151-159.

Bessonov, N., Morozova, N. and Volpert, V., 2008. *Modeling of Branching Pattern in Plants*. Bulletin of Mathematical Biology. 70: 868-893.

Bravais, L. and Bravais, A., 1837. *Essai sur la disposition des feuilles curvisériées*. Annales des Sciences Naturelles Botanique e t Biologie Végétale. 7: 42-110, 193-221, 291-348; 8: 11-42.

Briand, C., Posluszny, U. and Larson, D., 1991. *Differential Axis Architecture in* Thuja occidentalis *(Eastern White Cedar)*. Canadian Journal of Botany. 70: 340-348.

Carpenter, R., Copsey, L., Vincent, C., Doyle, S., Magrath, R. and Coen, E., 1995. *Control of Flower Development and Phyllotaxy by Meristem Identity Genes in* Anturrhinum. Plant Cell. 7: 2001-2011.

Church, A., 1904. *On the relation of Phyllotaxis to Mechanical Laws*. Williams and Norgate: London.

de Reuille, P., Bohn-Courseau, I., Ljung, K., Morin, H., Carraro, N., Godin, C. and Traas, J., 2006. *Computer Simulations Reveal Properties of the Cell-cell Signaling Network at the Shoot Apex in* Arabidopsis. Proceedings of the National Academy of Sciences of the United States of America. 103: 1627-1632.

Dengler, N., 1999. *Anisophylly and Dorsiventral Shoot Symmetry*. International Journal of Plant Sciences. 160 (suppl.): S67-S80.

Douady, S. and Couder, Y., 1992. *Phyllotaxis as a Physical Self-organized Growth Process*. Physical Review Letters. 68: 2098-2101.

Douady, S. and Couder, Y., 1996a. *Phyllotaxis as a Dynamical Self Organizing Process Part I: the Spiral Modes Resulting from Time-periodic Iterations*. Journal of Theoretical Biology. 178: 255-274.

Douady, S. and Couder, Y., 1996b. *Phyllotaxis as a Dynamical Self Organizing Process Part II: the Spontaneous Formation of a Periodicity and the Coexistence of Spiral and Whorled Patterns*. Journal of Theoretical Biology. 178: 275-294.

Douady, S. and Couder, Y., 1996c. *Phyllotaxis as a Dynamical Self Organizing Process Part III: the Simulation of the Transient Regimes of Ontogeny*. Journal of Theoretical Biology. 178: 295-312.

Dumais, J. and Steele, C., 2000. *New Evidence for the Role of Mechanical Forces in the Shoot Apical Meristem*. Journal of Plant Growth Regulation. 19: 7-18.

England, W. and Tolbert, R. 1964. *A Seasonal Study of the Vegetative Shoot Apex of* Myriophyllum heterophyllum. American Journal of Botany. 51: 349-353.

Erickson, R. and Meicenheimer, R., 1977. *Photoperiod Induced Change in Phyllotaxis in* Xanthium. American Journal of Botany. 64: 981-988.

Fleming, A. 2002. *Plant Mathematics and Fibonacci's Flowers*. Nature. 418: 723.

Fleming, A. 2005. *Formation of Primordia and Phylltotaxy*. Current Opinion in Plant Biology. 8: 53-58.

Fleming, A., McQueen-Mason, S., Mandel, T. and Kuhlemeier, C., 1997. *Induction of Leaf Primordia by the Cell Wall Protein Expansion*. Science. 276: 1415-1418.

Green, P., 1999. *Expression of Patterns in Plants: Combining Molecular and Calculus-based Biophysical Paradigms*. American Journal of Botany. 86: 1059-1076.

Guédès, M. and Dupuy, P., 1983. *From Decussation to Distichy, with Some Comments on Current Theories of Phyllotaxis*. Botanical Journal of the Linnean Society. 87: 1-12.

Hallé, F., Oldeman, R. and Tomlinson, P., 1978. *Tropical Trees and Forests: an Architectural Analysis*. Springer – Verlag: New York.

Harris, W., 1977. *Disclinations*. Scientific American. 237: 130-145.

Harris, W., 1978. *Dislocations, Disclinations and Dispirations: Distractions in Very Naughty Crystals*. South African Journal of Science. 74: 332-338.

Heisler, M. and Jönsson, H., 2006a. *Modeling Auxin Transport and Plant Development*. Journal of Plant Growth Regulation. 25: 302-312.

Heisler, M. and Jönsson, H., 2006b. *Computer Modeling of Plant Development*. Journal of Plant Growth Regulation. 25: 267-269.

Heisler, M., Ohno, C., Das, P., Sieber, P., Reddy, G., Long, G. and Meyerowitz, E. 2005. *Pattern of Auxin Transport and Gene Expression during Primordium Development Revealed by Live Imaging of the* Arabidopsis *Inflorescence Meristem*. Current Biology. 15: 1899-1911.

Hellwig, H., Engelmann, R. and Deussen, O., 2006. *Contact Pressure Models for Spiral Phyllotaxis and Their Computer Simulation*. Journal of Theoretical Biology. 240: 489-500.

Hofmeister, W., 1868. *Allgemeine Morphologie der Gewachse*. In: *Handbuch der Physiologischen Botanik*. Edited by Bary, A., Irmisch, T. and Sachs, J. Engelmann: Leipzig. Pp. 405-664.

Hotton, S., Johnson, V., Wilbarger, J., Zwieniecki, K., Atela, P., Golé, C. and Dumais, J., 2006. *The Possible and the Actual in Phyllotaxis: Bridging the Gap between Empirical Observations and Iterative Models*. Journal of Plant Growth Regulation. 25: 313-323.

Hutchinson, J., 1973. *The Families of Flowering Plants*. 3rd ed. Clarendon Press: Oxford.

Institute of Systematic Botany, University of Zürich, 2005. *Phyllotaxis: an E-learning Unit.* ISBN: 3-905677-06-7.

Ishida, Y. and Iyama, S., 1976. *Observations of Wedge Disclinations and Their Behavior in a Bubble Raft Crystals.* Acta Metallurgica et Materialia. 24: 417-423.

Itoh, J., Kitano, H., Matsuoka, M. and Nagato, Y., 2000. *Shoot Organization Genes Regulate Shoot Apical Meristem Organization and the Pattern of Leaf Primordium Initiation in Rice.* Plant Cell. 12: 2161-2174.

Jackson, D. and Hake, S., 1999. *Control of Phyllotaxis in Maize by the* abphyll *Gene.* Development. 126: 315-323.

Jean, R., 1988. *Number-theoretic Properties of Two-dimensional Lattices.* Journal of Number Theory. 29: 206-223.

Jean, R., 1994. *Phyllotaxis: a Systematic Study in Plant Morphogenesis.* Cambridge University Press: New York.

Jean, R., 1995. *Phyllotaxis: the Status of the Field.* Mathematical Biosciences. 127: 181-206.

Jean, R. and Barabé, D., 1998a. *Phyllotaxis – the Way ahead, a View on Open Questions and Directions of Research.* Journal of Biological Systems. 6: 95-126.

Jean, R. and Barabé, D., 1998b. *Symmetry in Plants.* World Scientific: Singapore.

Jean, R.V. and Barabé, D., 2001. *Application of Two Mathematical Models to the* Araceae*, a Family of Plants with Enigmatic Phyllotaxis*. Annals of Botany. 88: 173-186.

Jeune, B. and Barabé, D., 2004. *Statistical Recognition of Random and Regular Phyllotactic Patterns*. Annals of Botany. 94: 913-917.

Jönsson, H., Heisler, M., Shapiro, B., Meyerowitz, E. and Mjolsness, E., 2006. *An Auxin-driven Polarized Transport Model for Phyllotaxis*. Proceedings of the National Academy of Sciences of the United States of America. 103: 1633-1638.

Kramer, E., 2008. *Computer Models of Auxin Transport: a Review and Commentary*. Journal of Experimental Botany. 59: 45-53.

Kuhlemeier, C., 2007. *Phyllotaxis*. Trends in Plant Science. 49: 460-480.

Kuhlemeier, C. and Reinhardt, D., 2001. *Auxin and Phyllotaxis*. Trends in Plant Science. 6: 187-189.

Kwiatkowska, D., 1995. *Ontogenetic Changes of Phyllotaxis in* Anagallis arvensis *L.* Acta Societatis Botanicorum Poloniae. 64: 319-325.

Kwiatkowska, D., 1999. *Formation of Pseudowhorls in* Peperomia verticillata *(L.) A. Dietr. Shoots Exhibiting Various Phyllotactic Patterns*. Annals of Botany. 83: 675-685.

Kwiatkowska, D. and Dumais, J., 2003. *Growth and Morphogenesis at the Vegetative Shoot Apex of* Anagallis arvensis *L.* Journal of Experimental Botany. 54: 1585-1595.

Lacroix, C., Barabé, D. and Jeune, B., 2004. *Early Stages of Initiation of Two Types of Leaves in* Thuja occidentalis *(Eastern White Cedar)*. Canadian Journal of Botany. 82: 598-606.

Lacroix, C., Jeune, B. and Barabé, D., 2005. *Encasement in Plant Morphology: An Integrative Approach from Genes to Organisms*. Canadian Journal of Botany. 83: 1207-1221.

Levitov, L., 1991a. *Energetic Approach to Phyllotaxis*. Europhysics Letters. 14: 533-539.

Levitov, L., 1991b. *Phyllotaxis of Flux Lattices in Layered Superconductors*. Physical Review Letters. 66: 224-247.

Leyser, O. and Day, S., 2003. *Mechanisms in Plant Development*. Blackwell: Oxford.

Lyndon, R., 1978. *Phyllotaxis and the Initiation of Primordia during Flower Development in* Silene. Annals of Botany. 42: 1349-1360.

Maksymoych, R. and Erickson, R., 1977. *Phyllotactic Change Induced by Gibberellic Acid in* Xanthium. American Journal of Botany. 64: 33-44.

Meicenheimer, R., 1979. *Relationships between Shoot Growth and Changing Phyllotaxy of* Ranunculus. American Journal of Botany. 66: 557-569.

Meicenheimer, R., 1981. *Changes in* Epilobium *Phyllotaxy Induced by N-1-Naphthylphalamic Acid and α-4-Chlorophenoxyisobutyric Acid*. American Journal of Botany. 68: 1139-1154.

Meicenheimer, R., 1982. *Change in* Epilobium *Phyllotaxy during Reproductive Transition*. American Journal of Botany. 69: 1108-1118.

Meicenheimer, R., 1987. *Role of Stem Growth in* Linum usitatissimum *Leaf Trace Patterns.* American Journal of Botany. 74: 857-867.

Meicenheimer, R., 1998. *Decussate to Spiral Transitions in Phyllotaxis.* In: *Symmetry in Plants.* Edited by Jean, R. and Barabé, D. World Scientific: Singapore. Pp. 125-143.

Meicenheimer, R. and Zagórska-Marek, B., 1989. *Consideration of the Geometry of the Phyllotaxic Pattern Triangular Unit and Discontinuous Phyllotactic Transitions.* Journal of Theoretical Biology. 139: 359-368.

Meinhardt, H., 1984. *Models of Pattern Formation and Their Application to Plant Development.* In: *Positional Controls in Plant Development.* Edited by Barlow, P. and Carr, D. Cambridge University Press: Cambridge. Pp. 1-32.

Meinhardt, H., 2003. *Complex Pattern Formation by a Self-destabilization of Established Patterns: Chemotactic Orientation and Phyllotaxis as Examples.* Comptes Rendus Biologies. 326: 223-237.

Meinhardt, H., 2004. Out-of-phase Oscillations and Traveling Waves with Unusual Properties: the Use of Three-component Systems in Biology. Physica D. 199: 264-277.

Merks, R., Van de Peer, Y., Inzé, D. and Beemster, G., 2007. *Canalization without Flux Sensors: a Traveling-wave Hypothesis.* Trends in Plant Science. 12: 384-390.

Navarro, C., Efremova, N., Golz, J., Rubiera, R., Kuckenberg, M., Castillo, R., Tietz, R., Saedler, H. and Schwarz-Sommer, Z., 2004. *Molecular and Genetic Interactions between* Stylosa *and* Graminifolia *in the Control of* Antirrhinum *Vegetative and Reproductive Development.* Development. 131: 3649-3659.

Newell, A. and Shipman, P., 2005. *Plants and Fibonacci.* Journal of Statistical Physics. 121: 937-968.

Newell, A., Shipman, P. and Sun, Z., 2008. *Phyllotaxis: Cooperation and Competition between Mechanical and Biophysical Processes.* Journal of Theoretical Biology. 251: 421-439.

Nishimura, A., Ito, M., Kamiya, N., Sato, Y. and Matsuoka, M., 2002. OsPNH1 *Regulates Leaf Development and Maintenance of the Shoot Apical Meristem in Rice.* Plant Journal. 30: 189-201.

Nour, K., Yeung, E. and Thorpe, T. *Shoot Bud Histogenesis from Mature Embryos and Shoots of Eastern White Cedar (*Thuja occidentalis *L.) Cultured* in vitro. International Journal of Plant Sciences. 154: 378-385.

Otsuga, D., DeGuzman, B., Prigge, M., Drews, G. and Clark, S., 2001. REVOLUTA *Regulates Meristem Initiation at Lateral Positions.* Plant Journal. 25: 223-236.

Prusinkiewicz, P. and Rolland-Logan, A., 2006. *Modeling Plant Morphogenesis.* Current Opinion in Plant Biology. 9: 83-88.

Reinhardt, D., 2005. *Phyllotaxis – a New Chapter in an Old Tale about Beauty and Magic Numbers*. Current Opinion in Plant Biology. 8: 487-493.

Reinhardt, D., Frenz, M., Mandel, T. and Kuhlemeier, C., 2005. *Microsurgical and Laser Ablation Analysis of Leaf Positioning and Dorsoventral Patterning in Tamato*. Development. 132: 15-26.

Reinhardt, D. and Kuhlemeier, C., 2001. *Phyllotaxis in Higher Plants*. In: *Merismetic Tissues in Plant Growth and Development*. Edited by McManus, M. and Veit, B. Sheffield University Press: Sheffield. Pp. 172-212.

Reinhardt, D., Mandel, T. and Kuhlemeier, C., 2000. *Auxin Regulates the Initiation and Radial Position of Plant Lateral Organs*. Plant Cell. 12: 507-518.

Reinhardt, D., Pesce, E., Stieger, P., Mandel, T., Baltensperger, K., Bennett, M., Traas, J., Friml. J. and Kuhlemeier, C., 2003. *Regulation of Phyllotaxis by Polar Auxin Transport*. Nature. 426: 255-260.

Reinhardt, D., Witter, F., Mandel, T. and Kuhlemeier, C., 1998. *Localized Upregulation of a New Expansion Gene Predicts the Site of Leaf Formation in the Tomato Meristem*. Plant Cell. 10: 1427-1437.

Richards, F., 1948. *The Geometry of Phyllotaxis and Its Origin*. Symposium of the Society for Experimental Biology. 2: 217-245.

Richards, F., 1951. *Phyllotaxis: Its Quantitative Expression and Relation to Growth in the Apex.* Philosophical Transactions of the Royal Society of London. Series B, Biological Sciences. 235: 509-564.

Rutishauser, R., 1986. *Phyllotactic Patterns in Phyllodinous* Acacias *(*Acacia *subg.* heterophyllum*) – Promising Aspects for Systematics.* Bulletin of the International Group for the Study of Mimosoideae. 14: 77-108.

Rutishauser, R., 1998. *Plastochrone Ratio and Leaf Arc as Parameters of a Quantitative Phyllotaxis Analysis in Vascular Plants.* In: *Symmetry in Plants.* Edited by Jean, R. and Barabé, D. World Scientific: Singapore. Pp. 171-212.

Sattler, R., 1978. *Introduction.* In: *Theoretical Plant Morphology.* Edited by Sattler, R. Leiden University Press: Hague. Pp. 5-20.

Schwabe, W., 1971. *Chemical Modifications of Phyllotaxis and Its Implications.* Symposium of the Society for Experimental Biology. 25: 310-322.

Schwabe, W. and Clewer, A., 1984. *Phyllotaxis – A Simple Computer Model Based on the Theory of a Polarly-induced Inhibitor.* Journal of Theoretical Biology. 109: 595-619.

Schoute, J., 1913. *Beiträge zur Blattstellungslehre I. Die Theorie.* Recueil des Travaux Botaniques Néerlandais. 10: 153-339.

Schoute, J., 1925. *On whorled Phyllotaxis II. Late Binding Whorls of* Peperomia. Recueil des Travaux Botaniques Néerlandais. 22: 128-172.

Schoute, J., 1936. *On whorled Phyllotaxis III. True and False Whorls*. Recueil des Travaux Botaniques Néerlandais. 33: 670-687.

Shipman, P. and Newell, A., 2004. *Phyllotactic Patterns on Plants*. Physical Review Letters. 92: 168102.

Shipman, P. and Newell, A., 2005. *Polygonal Planforms and Phyllotaxis on Plants*. Journal of Theoretical Biology. 236: 154-197.

Shipman, P. and Newell, A., 2008. *A New Invariant in Plant Phyllotaxis*. Analysis and Applications. 6: 383-399.

Sinnott, E., 1960. *Plant Morphogenesis*. McGraw-Hill: New York.

Smith, R., 2008. *The Role of Auxin Transport in Plant Patterning Mechanisms*. PLOS Biology. 6: e323.

Smith, R., Guyomarc'h, S., Mandel, T., Reinhardt, D., Kuhlemeier, C. and Prusinkiewicz, P. 2006. *A Plausible model of Phyllotaxis*. Proceedings of the National Academy of Sciences of the United States of America. 103: 1301-1306.

Snow, M. and Snow, R., 1931. *Experiments on Phyllotaxis I. – The Effect of Isolating a Primordium*. Philosophical Transactions of the Royal Society of London. Series B, Containing Papers of a Biological Character. 221: 1-43.

Snow, M. and Snow, R., 1933. *Experiments on Phyllotaxis II. – The Effect of Displacing a Primordium.* Philosophical Transactions of the Royal Society of London. Series B, Containing Papers of a Biological Character. 222: 353-400.

Snow, M. and Snow, R., 1935. *Experiments on Phyllotaxis III. – Diagonal Splits through Decussate Apices.* Philosophical Transactions of the Royal Society of London. Series B, Biological Sciences. 225: 63-94.

Snow, M. and Snow, R., 1937. *Auxin and Leaf Formation.* New Phytologist. 36: 1-18.

Snow, M. and Snow, R., 1952. *Minimum Areas and Leaf Determination.* Proceedings of the Royal Society of London. Series B, Biological Sciences. 139: 545-566.

Snow, M. and Snow, R., 1962. *A Theory of the Regulation of Phyllotaxis Based on* Lupinus albus. Philosophical Transactions of the Royal Society of London. Series B, Biological Sciences. 244: 483-513.

Steeves, T. and Sussex, I., 1989. *Patterns in Plant Development.* 2nd ed. Cambridge University Press: New York.

Takahashi, T., Matsuhara, S., Abe., M. and Komeda, Y., 2002. *Disruption of a DNA Topoisomerase I Gene Affects Morphogenesis in* Arabidopsis. Plant Cell. 14: 2085-2093.

Tamaoki, M., Nishimura, A., Aida, M., Tasaka, M. and Matusoka, M., 1999. *Transgenic Tobacco Over-expressing a Homeobox Gene Shows a Developmental Interaction between Leaf Morphogenesis and Phyllotaxy.* Plant and Cell Physiology. 40: 657-667.

Traas. J. and Vernoux. T., 2002. *The Shoot Apical Meristem: the Dynamics of a Stable Structure.* Philosophical Transactions: Biological Sciences. 357: 737-747.

Turing, A., 1952. *The Chemical Basis of Morphogenesis.* Philosophical Transactions of the Royal Society of London. Series B, Biological Sciences. 237: 37-52.

van Iterson, G., 1907. *Mathematische und Mikroskopisch-Anatomische Studien über Blattstellungen nebst Betraschtungen über den Schalenbau der Miliolinen.* Gustav Fischer Verlag: Jena.

Veen, A. and Lindenmayer, A., 1977. *Diffusion Mechanism for Phyllotaxis, Theoretical, Physico-chemical and computer study.* Plant Physiology. 60: 127-139.

Veit, B., Briggs, S., Schmidt, R., Yanofsky, M. and Hake, S., 1998. *Regulation of Leaf Initiation by* terminal ear1 *Gene of Maize.* Nature. 393: 166-168.

Wardlaw, C., 1949. *Experiments on Organogenesis in Ferns.* Growth. 13 (suppl.): 93-131.

Williams, R., 1975. *The Shoot Apex and Leaf Growth: a Study in Quantitative Biology.* Cambridge University Press: New York.

Yamada, H., Tanaka, R. and Nakagaki, T., 2004. *Sequences of Symmetry-breaking in Phyllotactic Transitions.* Bulletin of Mathematical Biology. 66: 779-789.

Zagórska-Marek, B., 1985. *Phyllotactic Patterns and Transitions in* Abies balsamea. Canadian Journal of Botany. 63: 1844-1854.

Zagórska-Marek, B., 1987. *Phyllotaxis Triangular Unit; Phyllotactic Transitions as the Consequences of the Apical Wedge Disclinations in a Crystal-like Pattern of the Units.* Acta Societatis Botanicorum Poloniae. 56: 229-255.

Zagórska-Marek, B., 1994. *Phyllotaxic Diversity in* Magnolia *Flowers.* Acta Societatis Botanicorum Poloniae. 63: 117-137.

Zagórska-Marek, B. and Szpak, M., 2008. *Virtual Phyllotaxis and Real Plant Model Cases.* Functional Plant Biology. 35: 1025-1033.

Zagórska-Marek, B. and Wiss, D., 2003. *Dislocations in the Repetitive Unit Patterns of Biological Systems.* In: *Formal Descriptions of Developing Systems.* Edited by Nation, J., Trofimova, I., Rand, J. and Sulis, W. Kluwer Academic Press: Dordrecht. Pp. 99-117.

Appendix A: Recipes for the graded TBA series and the steps of dehydration

	Distilled water	95% ethanol	TBA	100% ethanol
TBA1	50ml	40ml	10ml	-
TBA2	30ml	50ml	20ml	-
TBA3	15ml	50ml	35ml	-
TBA4	-	45ml	55ml	-
TBA5	-	-	75ml	25ml

Step 1: TBA 1 at room temperature for 12h;

Step 2: TBA 2 at room temperature for 12h;

Step 3: TBA 3 at room temperature for 12h;

Step 4: TBA 4 at room temperature for 12h;

Step 5: TBA 5 at room temperature for 12h;

Step 6: pure TBA at 37C for 12h;

Step 7: pure TBA at 61C for 12h.

Appendix B: *Confection of the Haupt's solution*

Dissolve 1g gelatin in 100ml distilled water. When it is completely dissolved, stir into 2g phenol crystals and 15ml glycerin and then filter the solution.

Appendix C: The standard protocol of toluidine blue (TB) staining for histological sections

Step 1: 100% citrisolve at room temperature for 5min;

Step 2: 100% citrisolve at room temperature for 5min;

Step 3: 1:1 mixture of 100% citrisolve and 100% ethanol at room temperature for 5min;

Step 4: 100% ethanol at room temperature for 5min;

Step 5: 95% ethanol at room temperature for 5min;

Step 6: 70% ethanol at room temperature for 5min;

Step 7: 50% ethanol at room temperature for 5min;

Step 8: 1% toluidine blue (TB) at room temperature for 5min;

Step 9: distilled water at room temperature for 5min;

Step 10: distilled water at room temperature for 5min;

Step 11: 50% ethanol at room temperature for 5min;

Step 12: 70% ethanol at room temperature for 5min;

Step 13: 95% ethanol at room temperature for 5min;

Step 14: 100% ethanol at room temperature for 5min;

Step 15: 1:1 mixture of 100% citrisolve and 100% ethanol at room temperature for 5min;

Step 16: 100% citrisolve at room temperature for 5min;

Step 17: 100% citrisolve at room temperature for 5min.

Appendix D: Tables 11-19

Table 11: volume of the SAM (*v*), surface area of the SAM (*sa*), projected area of the SAM (*pa*) and height of the SAM (*h*) for the tetracussate pattern of the main stem of *T. occidentalis*.

	v (μm^3)	*sa* (μm^2)	*pa* (μm^2)	*h* (μm)
Apex 1	40381	6527	3723	46.77
Apex 2	35348	5261	3801	31.21
Apex 3	22842	3994	2670	25.17
Apex 4	46264	5565	3043	36.67
Apex 5	56737	6164	3575	34.62
Apex 6	81721	7991	4000	48.37
Apex 7	23254	4681	3636	20.42
Apex 8	23947	4065	2819	20.97
Apex 9	5024	2497	1969	18.43

Table 12: volume of the SAM (*v*), surface area of the SAM (*sa*), projected area of the SAM (*pa*) and height of the SAM (*h*) for the tricussate pattern of the main stem of *T. occidentalis*.

	v (μm^3)	*sa* (μm^2)	*pa* (μm^2)	*h* (μm)
Apex 1	24029	3873	2270	35.68
Apex 2	47711	5570	3018	34.17
Apex 3	22433	3589	2084	31.09
Apex 4	24981	3855	2236	30.80
Apex 5	36459	4593	2498	34.87
Apex 6	30325	4122	2312	27.96
Apex 7	66847	6928	3299	45.13
Apex 8	69654	7210	3724	41.58
Apex 9	42861	5174	2967	33.00
Apex 10	29416	4190	2545	29.51
Apex 11	28532	3887	2375	25.86
Apex 12	30334	4478	3051	23.37
Apex 13	55456	5913	3182	35.39
Apex 14	79833	7961	3716	49.53
Apex 15	55435	6057	3148	39.78
Apex 16	34111	4656	2825	26.62
Apex 17	22236	3664	2080	28.30
Apex 18	51088	5967	3146	41.50
Apex 19	36324	5442	3265	31.46

Table 12 continued

Apex 20	35153	4728	2654	35.17
Apex 21	42062	5279	2853	35.39
Apex 22	50601	5985	3229	39.28
Apex 23	28943	4305	2805	25.57
Apex 24	134539	11220	5733	53.85
Apex 25	65688	6898	3577	39.79

Table 13: volume of the SAM (*v*), surface area of the SAM (*sa*), projected area of the SAM (*pa*) and height of the SAM (*h*) for the (3, 5) spiral pattern of the main stem of *T. occidentalis*.

	v (μm^3)	sa (μm^2)	pa (μm^2)	h (μm)
Apex 1	19735	3368	2310	19.39
Apex 2	32843	4575	2751	30.46
Apex 3	49049	5728	3175	34.52
Apex 4	46978	5464	3143	31.13
Apex 5	56413	6353	3481	38.61

Table 14: volume of the SAM (*v*), surface area of the SAM (*sa*), projected area of the SAM (*pa*) and height of the SAM (*h*) for the decussate pattern of the main stem of *T. occidentalis*.

	v (μm^3)	*sa* (μm^2)	*pa* (μm^2)	*h* (μm)
Apex 1	21819	3499	2254	19.05
Apex 2	74711	8361	3655	56.32
Apex 3	59206	6569	3113	43.83
Apex 4	40617	4951	2382	37.88
Apex 5	35905	4597	2538	28.48
Apex 6	60552	6464	2963	42.63
Apex 7	37927	4799	2358	34.37
Apex 8	71762	7893	3719	49.45
Apex 9	29975	4277	2727	28.66
Apex 10	42266	5011	2544	35.03
Apex 11	38904	4813	2710	36.66
Apex 12	34711	4450	2503	30.17

Table 15: volume of the SAM (v), surface area of the SAM (sa), projected area of the SAM (pa) and height of the SAM (h) for the decussate pattern of the side branches of *T. occidentalis*.

	v (μm^3)	sa (μm^2)	pa (μm^2)	h (μm)
Apex 1	60813	6672	3293	38.65
Apex 2	58213	6676	2565	47.83
Apex 3	28108	4049	2014	31.12
Apex 4	18239	3361	2165	21.34
Apex 5	45848	5789	2446	43.51
Apex 6	40977	5522	2823	45.14
Apex 7	27766	5165	2198	56.49
Apex 8	34892	4973	2561	37.90
Apex 9	17594	3065	1659	31.52
Apex 10	22936	3818	2159	32.27
Apex 11	35729	5175	3001	30.68
Apex 12	42529	5544	3322	33.33
Apex 13	48072	6025	3221	35.93
Apex 14	60812	7033	3141	48.04
Apex 15	35500	4957	2463	34.13
Apex 16	34686	4775	2315	35.05
Apex 17	37328	4928	2357	34.07
Apex 18	34385	4426	2299	29.65
Apex 19	43897	5418	2398	40.27

Table 15 continued

Apex 20	47627	5991	2657	40.58
Apex 21	16502	2785	1485	22.61
Apex 22	47674	5739	2604	40.45
Apex 23	23083	3724	1709	35.64
Apex 24	40129	5112	2662	32.99
Apex 25	31897	4467	2511	29.38
Apex 26	22660	3749	2004	31.69
Apex 27	26963	4177	2149	38.27
Apex 28	45031	6044	2476	48.32
Apex 29	26065	3928	2073	31.37
Apex 30	15111	2733	1493	28.44
Apex 31	45604	5698	2552	47.77
Apex 32	21054	3386	1900	24.10
Apex 33	112851	9840	4637	50.40
Apex 34	30990	4337	2527	27.94
Apex 35	90521	9060	5333	44.53
Apex 36	56651	6166	3320	36.54
Apex 37	107530	9701	4297	59.09
Apex 38	30551	4253	2499	30.01
Apex 39	123805	10604	4487	58.81
Apex 40	112446	10162	4025	61.29

Table 15 continued

Apex 41	55588	6262	3456	34.28
Apex 42	44768	5371	3109	33.30
Apex 43	31304	4975	2564	36.19
Apex 44	47551	5689	3294	33.96
Apex 45	52739	5965	3011	39.65
Apex 46	80994	8287	4304	46.06
Apex 47	60887	6632	3612	38.14

Table 16: Values of parameter Γ calculated by 3 different equations.

	$\Gamma = l_1/R_0$	$\Gamma = \sqrt{(l_1 l_2)}/R_0$	$\Gamma = 2\sin(i_1/2)$		$\Gamma = l_1/R_0$	$\Gamma = \sqrt{(l_1 l_2)}/R_0$	$\Gamma = 2\sin(i_1/2)$
Primordium 1	0.89	0.55	1.16	Primordium 33	1.79	1.64	1.03
Primordium 2	0.74	0.47	1.29	Primordium 34	0.75	0.64	0.64
Primordium 3	1.19	0.86	1.21	Primordium 35	2.63	2.11	1.14
Primordium 4	0.96	0.60	0.99	Primordium 36	1.96	1.48	1.40
Primordium 5	2.15	1.75	1.15	Primordium 37	1.98	1.38	1.38
Primordium 6	2.58	2.10	1.48	Primordium 38	1.96	1.58	1.40
Primordium 7	2.75	2.29	1.48	Primordium 39	1.52	1.07	1.13
Primordium 8	2.27	1.97	1.44	Primordium 40	1.82	1.36	1.27
Primordium 9	1.44	1.43	0.89	Primordium 41	0.79	0.65	0.83
Primordium 10	1.54	1.36	1.24	Primordium 42	1.50	0.94	1.57
Primordium 11	1.04	0.97	0.86	Primordium 43	0.88	0.51	0.86
Primordium 12	1.74	1.54	1.22	Primordium 44	1.77	1.28	1.39
Primordium 13	0.95	0.69	1.09	Primordium 45	1.16	0.97	0.83
Primordium 14	1.03	0.72	1.14	Primordium 46	1.11	0.71	1.21
Primordium 15	1.04	0.77	1.13	Primordium 47	1.24	0.83	1.38
Primordium 16	0.96	0.76	1.19	Primordium 48	1.67	1.20	1.31
Primordium 17	1.89	1.64	1.29	Primordium 49	1.02	0.77	0.82
Primordium 18	1.65	1.34	1.14	Primordium 50	1.07	0.70	0.97
Primordium 19	1.49	1.25	0.98	Primordium 51	1.12	0.67	1.24
Primordium 20	0.32	0.26	0.24	Primordium 52	1.36	0.93	1.63

Table 16 continued

Primordium 21	1.36	1.17	1.28	Primordium 53	1.23	0.93	1.41
Primordium 22	1.07	0.94	0.61	Primordium 54	2.37	2.23	1.74
Primordium 23	1.25	0.99	1.18	Primordium 55	2.43	2.34	1.66
Primordium 24	0.92	0.71	1.07	Primordium 56	1.37	1.15	1.01
Primordium 25	1.08	0.87	1.11	Primordium 57	1.59	1.21	1.36
Primordium 26	1.70	1.35	1.39	Primordium 58	1.45	1.16	1.16
Primordium 27	1.13	0.94	0.69	Primordium 59	1.57	1.23	1.29
Primordium 28	1.42	1.28	1.10	Primordium 60	1.42	1.11	1.11
Primordium 29	1.15	0.93	0.72	Primordium 61	1.39	1.03	1.04
Primordium 30	1.41	1.14	1.06	Primordium 62	1.01	0.57	0.84
Primordium 31	1.18	0.94	0.84	Primordium 63	1.38	0.95	1.11
Primordium 32	0.81	0.75	0.68				

Table 17: comparison of plastochrone ratio (R) for true whorl and corresponding pseudowhorl. Apices 1-5: true tricussate pattern; apices 6-19: true decussate pattern (regardless whether it is main stem or side branches).

	R value of true whorl	R value of pseudowhorl
Apex 1	1.16	1.17
Apex 2	1.15	1.17
Apex 3	1.16	1.16
Apex 4	1.16	1.17
Apex 5	1.14	1.15
Apex 6	1.18	1.23
Apex 7	1.23	1.30
Apex 8	1.17	1.22
Apex 9	1.18	1.24
Apex 10	1.23	1.29
Apex 11	1.20	1.26
Apex 12	1.23	1.30
Apex 13	1.21	1.29
Apex 14	1.28	1.34
Apex 15	1.21	1.27
Apex 16	1.21	1.27
Apex 17	1.21	1.27
Apex 18	1.19	1.28
Apex 19	1.19	1.23

Table 18: fluctuation of plastochrone ratio (R) values around their mean values with a period of 2 plastochrones for the groups "first pair of leaves elongated in the radial direction" and "first pair of leaves elongated in the tangential direction" of decussate pattern of the side branches of *T. occidentalis*. Apex numbers corresponds to table 5. Apices 5-7: first pair of leaves elongated in the radial direction; apices 8-10: first pair of leaves elongated in the tangential direction.

	R_{12}	R_{23}	R_{34}	R_{45}	R_{mean}
Apex 5	1.15	1.34	1.14	1.32	1.23
Apex 6	1.22	1.50	0.99	1.51	1.28
Apex 7	1.15	1.32	1.14	1.26	1.21
Apex 8	1.26	1.19	1.34	1.02	1.20
Apex 9	1.34	1.20	1.37	1.05	1.23
Apex 10	1.27	1.17	1.46	0.98	1.21

Table 19: measured values from the SEM 3D reconstruction of the SAM and calculated values from the equations established of the cone for volume of the SAM (v), surface area of the SAM (sa), height of the SAM (h) and apical angle of the SAM (ψ) for each apex from various phyllotactic patterns of *T. occidentalis*. Apices 1-9: tetracussate pattern of the main stem; apices 10-34: tricussate pattern of the main stem; apices 35-39: (3, 5) spiral pattern of the main stem; apices 40-51: decussate pattern of the main stem; apices 52-98: decussate pattern of the side branches.

	v (μm^3)		sa (μm^2)		h (μm)		ψ
	measured	calculated	measured	calculated	measured	calculated	calculated
Apex 1	40381	58042	6527	6281	46.77	32.54	93.23°
Apex 2	35348	39543	5261	5107	31.21	27.90	102.54°
Apex 3	22842	22401	3994	3527	25.17	25.67	97.28°
Apex 4	46264	37196	5565	4703	36.67	45.61	68.62°
Apex 5	56737	41256	6164	5123	34.62	47.61	70.64°
Apex 6	81721	64493	7991	6738	48.37	61.29	60.41°
Apex 7	23254	24749	4681	4241	20.42	19.19	121.16°
Apex 8	23947	19705	4065	3441	20.97	25.48	99.22°
Apex 9	5024	12096	2497	2445	18.43	7.65	146.00°
Apex 10	24029	26998	3873	3772	35.68	31.76	80.49°
Apex 11	47711	34375	5570	4492	34.17	47.43	66.33°
Apex 12	22433	21597	3589	3267	31.09	32.29	77.15°
Apex 13	24981	22956	3855	3415	30.80	33.52	77.04°
Apex 14	36459	29035	4593	3973	34.87	43.79	65.56°
Apex 15	30325	21548	4122	3320	27.96	39.35	69.17°

Table 19 continued

Apex 16	66847	49628	6928	5656	45.13	60.79	56.12°
Apex 17	69654	51615	7210	5839	41.58	56.11	63.07°
Apex 18	42861	32637	5174	4354	33.00	43.34	70.68°
Apex 19	29416	25034	4190	3666	29.51	34.68	78.76°
Apex 20	28532	20473	3887	3260	25.86	36.04	74.68°
Apex 21	30334	23767	4478	3814	23.37	29.83	92.51°
Apex 22	55456	37537	5913	4759	35.39	52.28	62.66°
Apex 23	79833	61351	7961	6515	49.53	64.45	56.17°
Apex 24	55435	41742	6057	5056	39.78	52.83	61.86°
Apex 25	34111	25067	4656	3778	26.62	36.22	79.24°
Apex 26	22236	19621	3664	3092	28.30	32.07	77.48°
Apex 27	51088	43520	5967	5188	41.50	48.72	66.01°
Apex 28	36324	34239	5442	4562	31.46	33.38	88.01°
Apex 29	35153	31114	4728	4166	35.17	39.74	72.37°
Apex 30	42062	33656	5279	4401	35.39	44.23	68.54°
Apex 31	50601	42278	5985	5107	39.28	47.01	68.58°
Apex 32	28943	23908	4305	3692	25.57	30.96	87.98°
Apex 33	134539	102907	11220	9225	53.85	70.40	62.50°
Apex 34	65688	47443	6898	5531	39.79	55.09	62.97°
Apex 35	19735	14930	3368	2840	19.39	25.63	93.23°
Apex 36	32843	27932	4575	3948	30.46	35.82	79.13°

Table 19 continued

Apex 37	49049	36534	5728	4687	34.52	46.35	68.90°
Apex 38	46978	32614	5464	4410	31.13	44.84	70.40°
Apex 39	56413	44800	6353	5331	38.61	48.62	68.80°
Apex 40	21819	14313	3499	2766	19.05	29.04	85.37°
Apex 41	74711	68617	8361	7056	56.32	61.32	58.17°
Apex 42	59206	45481	6569	5337	43.83	57.06	57.77°
Apex 43	40617	30077	4951	4051	37.88	51.15	56.59°
Apex 44	35905	24094	4597	3593	28.48	42.44	67.62°
Apex 45	60552	42104	6464	5069	42.63	61.31	53.21°
Apex 46	37927	27015	4799	3783	34.37	48.25	59.17°
Apex 47	71762	61302	7893	6512	49.45	57.89	61.45°
Apex 48	29975	26052	4277	3804	28.66	32.98	83.56°
Apex 49	42266	29705	5011	4035	35.03	49.84	59.45°
Apex 50	38904	33116	4813	4334	36.66	43.07	68.59°
Apex 51	34711	25172	4450	3664	30.17	41.60	68.31°
Apex 52	60813	42425	6672	5128	38.65	55.40	60.60°
Apex 53	58213	40895	6676	5001	47.83	68.09	45.53°
Apex 54	28108	20892	4049	3191	31.12	41.87	62.33°
Apex 55	18239	15400	3361	2790	21.34	25.27	92.17°
Apex 56	45848	35475	5789	4531	43.51	56.23	52.78°
Apex 57	40977	42477	5522	5103	45.14	43.55	69.09°

Table 19 continued

Apex 58	27766	41388	5165	5183	56.49	37.90	69.83°
Apex 59	34892	32354	4973	4256	37.90	40.87	69.87°
Apex 60	17594	17431	3065	2816	31.52	31.82	71.68°
Apex 61	22936	23224	3818	3424	32.27	31.87	78.88°
Apex 62	35729	30690	5175	4228	30.68	35.72	81.74°
Apex 63	42529	36907	5544	4757	33.33	38.41	80.51°
Apex 64	48072	38577	6025	4841	35.93	44.77	71.14°
Apex 65	60812	50298	7033	5713	48.04	58.08	57.13°
Apex 66	35500	28021	4957	3883	34.13	43.24	65.85°
Apex 67	34686	27047	4775	3781	35.05	44.95	62.26°
Apex 68	37328	26768	4928	3762	34.07	47.51	59.93°
Apex 69	34385	22722	4426	3411	29.65	44.87	62.17°
Apex 70	43897	32189	5418	4239	40.27	54.92	53.41°
Apex 71	47627	35940	5991	4561	40.58	53.78	56.81°
Apex 72	16502	11192	2785	2142	22.61	33.34	66.22°
Apex 73	47674	35111	5739	4491	40.45	54.92	55.33°
Apex 74	23083	20303	3724	3121	35.64	40.52	59.85°
Apex 75	40129	29273	5112	4023	32.99	45.22	65.54°
Apex 76	31897	24591	4467	3621	29.38	38.11	73.14°
Apex 77	22660	21169	3749	3215	31.69	33.92	73.34°
Apex 78	26963	27414	4177	3809	38.27	37.64	69.59°

Table 19 continued

Apex 79	45031	39880	6044	4929	48.32	54.56	54.46°
Apex 80	26065	21677	3928	3272	31.37	37.72	68.51°
Apex 81	15111	14154	2733	2454	28.44	30.36	71.35°
Apex 82	45604	40636	5698	4981	47.77	53.61	55.99°
Apex 83	21054	15263	3386	2660	24.10	33.24	72.99°
Apex 84	112851	77902	9840	7649	50.40	73.01	55.51°
Apex 85	30990	23535	4337	3547	27.94	36.79	75.26°
Apex 86	90521	79159	9060	7853	44.53	50.92	77.95°
Apex 87	56651	40438	6166	4995	36.54	51.19	64.83°
Apex 88	107530	84637	9701	8099	59.09	75.07	52.45°
Apex 89	30551	24998	4253	3649	30.01	36.68	75.12°
Apex 90	123805	87960	10604	8300	58.81	82.78	49.08°
Apex 91	112446	82231	10162	7981	61.29	83.81	46.25°
Apex 92	55588	39491	6262	4970	34.28	48.25	69.01°
Apex 93	44768	34510	5371	4527	33.30	43.20	72.13°
Apex 94	31304	30930	4975	4138	36.19	36.63	75.91°
Apex 95	47551	37288	5689	4773	33.96	43.31	73.57°
Apex 96	52739	39795	5965	4893	39.65	52.55	61.01°
Apex 97	80994	66081	8287	6871	46.06	56.45	66.50°
Apex 98	60887	45921	6632	5436	38.14	50.57	67.68°